Universitetet i Stavanger

DET TEKNISK-NATURVITENSKAPELIGE FAKULTET

BACHELOROPPGAVE

Studieprogram/spesialisering: Bachelor i biologisk kjemi	Vårsemesteret, 2021 Åpen / Konfidensiell
Forfatter: Elisabeth Lassa, Hedvig Svensson	
Fagansvarlig: Cathrine Lillo **Veileder(e):** Hanne Røland Hagland	
Tittel på bachelorpppgaven: Metformins effekt på bukspyttkjertel kreftcellenelinjene Panc-1 og MIA-Pa-Ca-2 **Engelsk tittel**: Metformin effect in the pancreatic cancer cell lines Panc-1 and MIA-Pa-Ca-2	
Studiepoeng: 20	
Emneord: Metformin, pancreatic cancer, machine learning, warburg effect, Panc-1, MIA-Pa-Ca-2	**Sidetall:** 44 **+ vedlegg/annet:** 3 Stavanger, 14.05/2021 dato/år

Metformin effect in the pancreatic cancer cell lines Panc-1 and MIA-Pa-Ca-2

Acknowledgement

We want to thank Hanne Røland Hagland for the opportunity to work with her team and for being assigned this project. We also want to thank Julie Nikolaisen for training us in advance of the experiments in the lab and Abdelnour Alhourani for machine learning training.

Abbreviations

OCR – Oxygen consumption rate

ECAR – Extracellular acidification rate

mTOR- mechanistic target of rapamycin

WST-8 - 2-(2-methoxy-4-nitrophenyl)-3-(4-nitrophenyl)-5-(2,4- disulfophenyl)-2H-tetrazolium, monosodium salt

ETC – Electron Transport Chain

TCA – the citric acid cycle

NADPH - nicotinamide dinucleotide phosphate

PPP - pentose phosphate pathway

AMPK - LKB1-AMP-activated protein kinase

AMP – adenosine mono phosphate

ATP – adenosine tri phosphate

ADT – androgen derivatives

NADH – Nicotinamide adenine dinucleotide

NAD+ - oxidized nicotinamide adenine dinucleotide

$FADH_2$ – reduced flavin adenine dinucleotide

PBS - Phosphate buffered saline

Acetyl CoA – Acetyl coenzyme A

mtDNA – mitochondria DNA

FCCP - Carbonyl cyanid-4 (trifluoromethoxy) phenylhydrazone

Contents

Abstract

This collaboration bachelor thesis focuses on cancer and how the drug metformin might be a future cancer treatment as it interrupt the cells metabolism by inhibition of complex I of the respiratory chain and numerous studies have shown that it affect cancer cells in many beneficial ways.

There are numerous publications available regarding metformin effect in cancer cells, and part of our bachelor thesis involved extracting data from 66 scientific articles where metformin was used and cells were tested for viability, oxygen consumption rates (OCR) and extracellular acidification rates (ECAR) and more, which we organized in a database. The database now includes information of which glucose concentration was used in cell growth media, metformin concentration, which cell lines were used, viability before and after metformin treatment, treatment time and the results of the XF seahorse analyzer; OCR and ECAR which are measurements of cell metabolism.

The aim was to use these data to create a model, using machine learning, that could predict cell how different cells would respond to metformin (viability) based on their metabolic data. Furthermore, we used two pancreatic cancer cell lines, Panc-1 and MIA-Pa-Ca-2 in lab experiments to test their sensitivity to metformin treatment using two different cell viability assays.

The two different pancreatic cancer cell lines, Panc-1 and MIA-Pa-Ca-2 was exposed to the biguanide drug metformin in three different concentrations. To be within the sensitivity of the assay, three cell viability assays was done in advance of the metformin experiment and showed that 10 000 cell/well was the best option. Both cell lines were seeded out as 10 000 cell/well on a 96-well plate before exposure to metformin. The cells were treated with three different metformin concentrations, 1 mM, 5 mM and 10 mM respectively, and incubated for 24 hours and 48 hours.

The results from the metformin treatment of the two cell lines showed that metformin does affect the cells as the cell viability decreased when the metformin concentration increased. The cells that was treated for 24 hours had much higher viability than those treated for 48 hours, so the most efficient treatment time was 48 hours. There were some deviations, especially for the Panc-1 cell line, but this was most likely due to errors done when preparing the plates. The MIA-Pa-Ca-2 cell line seemed to be more affected by 48 hours metformin treatment than Panc-1 cells, but the Panc-1 cells were more affected by 24 hours metformin treatment compared to MIA-Pa-Ca-2 cells based on results from this experiment.

The machine learning part was not very successful as the model did not give good predictions compared to the result. These results might have been different if done by someone with more experience. Machine learning have great protentional for medical research.

1. Introduction

1.1 Cancer

Cancer is the name of a collection of diseases that occurs when cells undergo abnormal cell growth and proliferation and spread to surrounding tissues. Cancer is one of the leading causes of death by disease in the world, so trying to understand this disease is a large field in science. In recent decades, the understanding of cancer diseases has developed at an incredible pace (Nature 2021) and the development and discovery of new treatments is improving rapidly. Understanding our cell's life cycle and metabolism is crucial for understanding the development of cancer. The cells in our bodies are highly complex and their life cycles involve numerous of regulations. When these regulations are disrupted, the normal cell processes break down and cancers may develop. Cancer is a genetic disease, changes and mutations in the cells genetics that controls certain functions, especially the cells life cycle, can cause cancer (National Cancer Institute 2021b).

The etiology of cancer is still being researched, but carcinogens such as cigarettes or radiation are well known to trigger cancer development. Other factors that might cause cancers are viruses and other infections, alcohol, poor diet, and little activity. Since cancer is a genetic disease, it can also be inherited and thus make some individuals more prone to develop cancer. The disease occurs in all age groups, but aging is definitively a risk factor. The elderly population is at greater risk for developing the disease. Cancer cells can develop in any kinds of tissues in the body, but the most common cancers are lung, breast, and prostate cancer. There are many different cancer therapies available, the most common being surgery, radiation, and chemotherapy. Some also gets targeted therapy, immunotherapy (see figure 1.1) laser, hormonal therapy and others (MedlinePlus Medical Encyclopedia 2021).

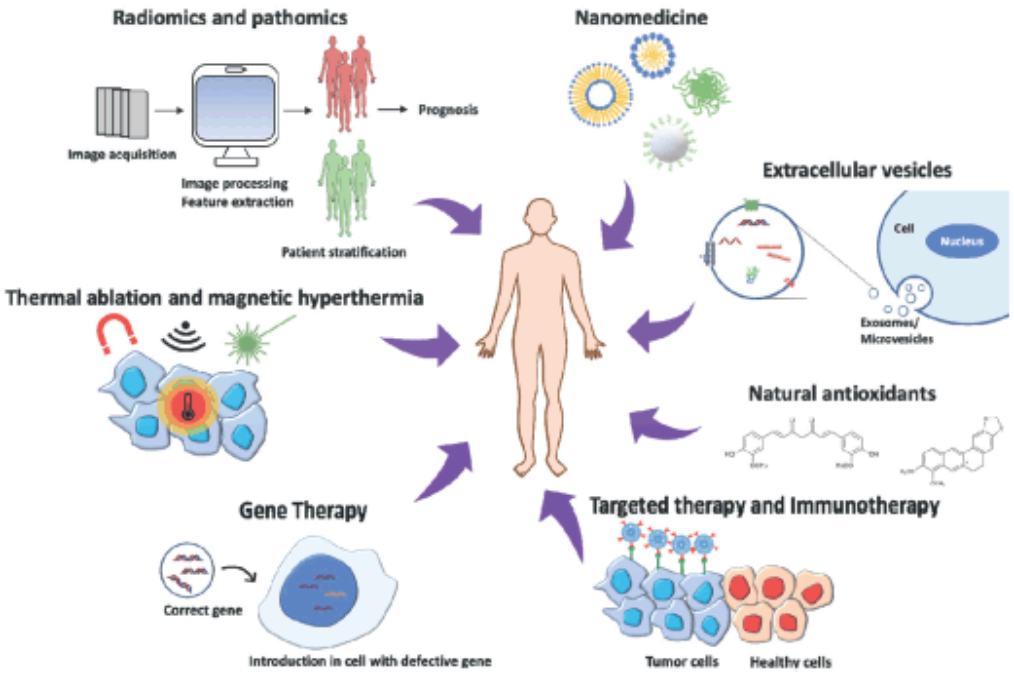

Figure 1.1: Cancer therapy approaches (Ecancer 2021)

This figure shows the most innovative cancer therapies, different disciplines combined to get the most efficient and personalized therapy for the patient. These therapies are radiomics and pathomics, nanomedicine, extracellular vesicles, natural antioxidants, targeted therapy and immunotherapy, gene therapy, thermal and magnetic hyperthermia (Ecancer 2021).

In this project our focus will be on pancreatic cancer which is one of the deadliest types of cancer. This aggressive cancer has the highest mortality rate in developed countries. It is more common for patients over 60 to get this type of cancer than middle age patients. The median age are 73 years. (Sarnecka et al. 2016).
Pancreatic cancer normally occurs for two reasons, environmental and genetic risk factors. The environmental can be smoking, diabetes, high fat consumption and alcohol abuse. Genetic risk factors can be age, family history, ethnicity and genetic factors. (Rawla et al. 2019).

1.1.1 The pancreas and pancreatic cancer

The pancreas lies behind the stomach in the upper abdomen. It looks like a 15 centimeters long pear on the side, the bigger part is called head, the middle part is called body and the thin last part is called tail (National Cancer Institute 2021a)

The pancreas is a gland, and its two main functions are control energy consumption and metabolism. The organ has two parts, one part is the exocrine pancreas and the other is the endocrine islets. The exocrine pancreas is a reservoir of digestive enzymes and the endocrine islets are the source of the vital metabolic hormone insulin (Zhou and Melton 2018).

The exocrine pancreas produces acinar cells and ductal cells. Acinar cells produce among other lipases, proteinases and amylases. These are secreted and transported to the intestine to break down fat, proteins and carbohydrates.

The endocrine pancreas constitutes less than 5% of the whole pancreas. This endocrine part of the pancreas also has more than a billion cells, and the major cells that gets synthesized and secrets are insulin, glucagon, somatostatin, pancreatic polypeptide and ghrelin. Insulin and glucagon are released directly into the blood system to regulate the blood glucose levels (Zhou and Melton 2018)

There are two tumor types of pancreatic cancer that are the most common, it is adenocarcinoma who is in the exocrine part (around 85% of the cases) and pancreatic endocrine tumor (less than 5% of the cases) (Rawla et al. 2019). The endocrine tumors are called pancreatic neuroendocrine tumors.

In this project there was studied two pancreatic cancer cell-lines. The first one is Panc-1 from a 56 year old male, the growth properties were adherent. The other cell-line we used were MIA-Pa-Ca-2 from a 65 year old Caucasian male, also here the growth properties was adherent. Both cell-lines were epithelial, see figure 1.2.

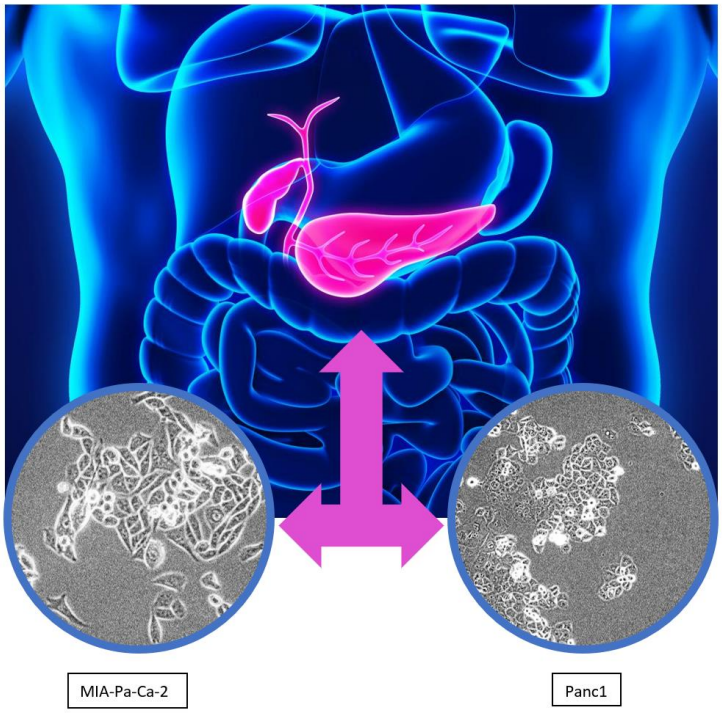

Figure 1.2: Location of pancreas in the abdomen (Medicalnewstoday 2020) and picture of two pancreatic cell lines

This figure shows the location of the pancreas in the abdomen and microscope pictures of the two pancreatic cells lines Panc-1 (to the right) and Mia-Pa-Ca-2 (to the left). This pancreas is the pink colored organ in the figure (Medicalnewstoday 2020).

1.1.2 Cancer metabolism

Cancer cells alter their metabolism to grow and proliferate rapidly, so they need to utilize glucose for generation of adenosine tri phosphate (ATP) differently than normal healthy cells, a phenomenon known as the Warburg effect (Warburg et al. 1927). In this section we will describe the basics in how normal cells utilize glucose, and then see how cancer cells adapt and changes their metabolic activity to support anabolic growth.

1.1.3 Normal cell metabolism

Normally cells utilize glucose by cellular respiration, that can be divided into four main steps. That is glycolysis, pyruvate oxidation, the citric acid cycle (TCA-cycle) and oxidative phosphorylation. In glycolysis the six-carbon sugar glucose is converted into two molecules of pyruvate, a three-carbon molecule. Glycolysis requires energy in the form of two ATP, and it generates four ATP, giving a net production of two ATPs. Glycolysis also converts two molecules of oxidized nicotinamide adenine dinucleotide (NAD+) to Nicotinamide adenine dinucleotide (NADH). In the absence of oxygen, the pyruvates formed through glycolysis gets rerouted into a process called fermentation. This process requires more NAD+ to keep the glycolysis process going. Thus, fermentation frees up some of the NAD+, resulting in the product lactic acid. If oxygen is present, the two molecules of pyruvate produced in glycolysis goes into the mitochondrial matrix where its converted into a two-carbon molecule bound to Coenzyme A (acetyl CoA). Here carbon dioxide is released and NADH is also generated. In the citric acid cycle, the acetyl CoA created by pyruvate oxidation combines with a four-carbon molecule, and then it goes through a large series of reactions and ends up with

regenerating the four-carbon molecule the circle started with, which can enter a new cycle. This cycle of reactions produces ATP, NADH and reduced flavin adenine dinucleotide ($FADH_2$) and releases carbon dioxide. The last step in cellular respiration is oxidative phosphorylation. This is where most of the ATP is produced. The NADH and $FADH_2$ produced in the earlier steps now deposit their electrons into the electron transport chain, see figure 1.3. The electrons move down a chain of complexes, releasing energy which is used to pump protons out of the mitochondrial matrix, and into the intermembrane space, creating a gradient. The protons then flow back into the matrix through the enzyme ATP-synthase and ATP are produced. In the end of the chain, oxygen molecules accept the electrons and takes up protons forming water molecules. Oxidative phosphorylation produces up to 36 ATP molecules per glucose molecule (Khan Academy 2021).

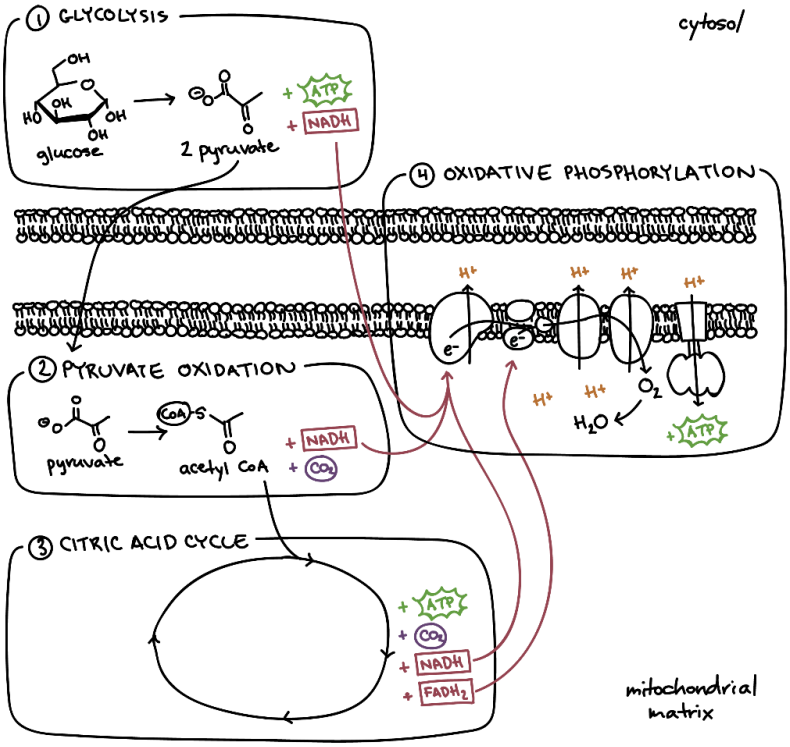

Figure 1.3: Normal cell metabolism (Khan Academy 2021)

This figure shows the main basic steps of how normal cells utilize glucose for energy production through aerobic glycolysis, pyruvate oxidation, the TCA cycle and at last oxidative phosphorylation in the electron transport chain. In glycolysis the glucose molecule undergoes a series of chemical transformations and is converted into two molecules of pyruvate, this process requires ATP and produces ATP and NADH. The pyruvate is then oxidized in the mitochondrial matrix and converted into a two-carbon molecule bound to acetyl-CoA. CO_2 is released and NADH is generated. In the citric acid cycle the acetyl-CoA is combined with a four-carbon molecule and undergo a series of reactions that regenerates the four-carbon molecule that can combine with a new acetyl-CoA and enter the cycle again. The TCA cycle produces ATP, NADH and $FADH_2$ and CO_2 is released. Oxidative phosphorylation in the last step in the series of reactions in cells utilization of glucose, and this is where the most ATPs are produced. It occurs in the inner membrane of the mitochondria. The NADH and the $FADH_2$ releases electrons into the electron transport chain. As the electrons moves down the chain, energy is released and protons are pumped into the intermembrane space of the mitochondria, creating an electrochemical gradient between the mitochondria matrix and intermembrane space. The protons flow back into the matrix trough the enzyme ATP synthase, making ATP. At the end of the electron transport chain oxygen accepts electrons and take up protons to form H_2O (Khan Academy 2021).

1.1.4 Cancer metabolism – the Warburg effect

Cancer cells on the other hand alter their metabolism to proliferate rapidly. The common feature of cancer cells altered metabolism is the increased glucose uptake and fermentation of glucose to lactate, even if they have a fully functionating mitochondria and when oxygen is present. This phenomenon is known as the Warburg effect and was discovered by the Nobel prize winner Otto Warburg in the 1920s (Warburg et al. 1927). The question is, why do proliferating cells switch to a less efficient way to produce ATP? Compared to the amount of ATP generated through mitochondrial respiration, per unit glucose, aerobic glycolysis is inefficient, but the rate of glucose metabolism in aerobic glycolysis is higher. That is, production of lactate from glucose occurs 10-100 times faster than the complete oxidation of glucose in the mitochondria (Liberti and Locasale 2016). Hence, this way of producing ATP is comparable to complete oxidation of glucose in the mitochondria. A theory is that cells with a higher rate, but lower yield of ATP production might have selective advantages when competing for nutrients (Liberti and Locasale 2016). A study found that when changes to the cells environment were exposed to greatly increase in ATP demand by altering the demand of ATP-dependent membrane pumps, aerobic glycolysis increased rapidly and oxidative phosphorylation remained constant (Liberti and Locasale 2016). This supports the supposed advantages of aerobic glycolysis in cancer cells. These metabolic alterations enable cancer cells to live in conditions of fluctuating oxygen tension that would be lethal for cells that rely on oxidative phosphorylation (Kroemer and Pouyssegur 2008).

When cancer cells generate lactic acid through glycolysis, such acidic conditions change their environment, and thus favor tumor invasion and even suppresses anticancer immune effectors. Stromal cells can take up lactic acid produced by tumor cells which regenerate pyruvate that can be used to refuel cancer cells or can be used in oxidative phosphorylation (Kroemer and Pouyssegur 2008). This generates a microecosystem where anaerobic and aerobic components engage in complementary metabolic pathways and recycles products of anaerobic metabolism. This sustains cancer cells survival and proliferation (Kroemer and Pouyssegur 2008). Tumors can also generate nicotinamide dinucleotide phosphate (NADPH) through the pentose phosphate pathway (PPP) by metabolizing glucose. NADPH ensures cells antioxidant defense and therefore protects the cells (Kroemer and Pouyssegur 2008). NADPH is also used for fatty acid synthesis (Kroemer and Pouyssegur 2008). Cancer cells use a large amount of glucose as a carbon source for anabolic reactions, and they can also use intermediates of the glycolytic pathway (Kroemer and Pouyssegur 2008). All these alterations help cancer cells to survive and divide in nutrient deplete conditions and proliferate rapidly.

Tumor mitochondria are usually relatively small, lack cristae and are deficient in the β-F1 unit of the ATP-synthase, which defects the oxidative phosphorylation and can help to explain the mechanisms of metabolic reprogramming of cancer cells (Kroemer and Pouyssegur 2008). However, the molecular mechanisms that underlie metabolic reprogramming of cancer cells are very complex. Mitochondria DNA (mtDNA) mutations might contribute to tumor progression or be a result of tumor progression. Expression on mutant mtDNA-encoded NADH dehydrogenase subunit 2 as a nuclear, mitochondria-targeted gene product stimulates aerobic glycolysis, production on reactive oxygen species and tumor growth (Kroemer and Pouyssegur 2008).

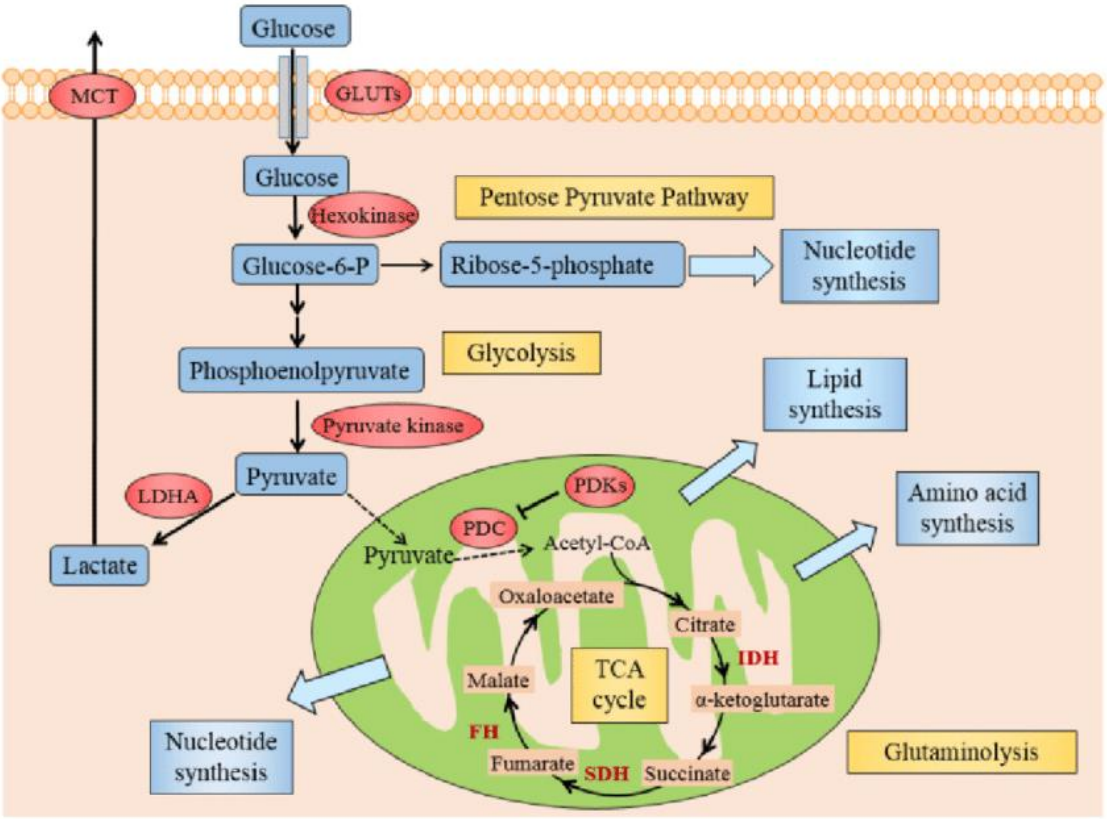

Figure 1.4: Illustration of the Warburg effect (Zhang et al. 2015).

This figure shows the prominent aspects of the Warburg effect like glycolysis, TCA cycle, lactate fermentation, glutamine metabolism, penthouse pyruvate pathway and the intermediates of the TCA cycle used to synthesize lipids, nucleotides and amino acids. The yellow boxes show pivotal metabolic pathways and the red circles illustrates the enzymes controlling key steps. Abbreviations: GLUTs: glucose transporters; MCT: monocarboxylate transporter; PDC: pyruvate dehydrogenase complex; PDKs: pyruvate dehydrogenase kinases; LDHA: lactate dehydrogenase A; HIF1: hypoxia inducible factor 1, IDH: isocitrate dehydrogenase; SDH: succinate dehydrogenase, FH: fumarate hydratase (Zhang et al. 2015).

1.2 Metformin

Metformin is a widely used biguanide drug used to treat type 2 diabetes due to its ability to decrease plasma glucose. It has been used for over 60 years, has few side effects and is considered safe, moreover it has relatively low cost. Discovery of the different effects of metformin have encouraged researchers to further study the drug, to see if it might have therapeutic effect on a variety of other diseases (Lv and Guo 2020). It is stated that metformin has shown benefits in diseases including cancers such as breast cancer, endometrial cancer, bone cancer, colorectal cancer and melanoma (Lv and Guo 2020). Metformin also showed benefits in diseases such as obesity, liver diseases, cardiovascular disease, renal disease and even in aging (Lv and Guo 2020).

Metformin is a derivate of galegine which is a natural product from the plant *Galega officinalis* that have been used as an herbal medicine in medieval Europe. In the 1920s galegine was found to be a glucose-lowering agent but was also found to be toxic. In this period both Metformin and Phenformin were synthesized and tested, and in 1950 they were introduced to clinical use. Galegine is chemically an isoprenyl derivate of guanidine. Metformin and Phenformin are biguanides containing two coupled molecules of guanidine with additional substitutions, see figure 1.5 (Rena et al. 2017).

Studies show that physiologically, metformin reduce gluconeogenesis, but not all its effect can be explained by this (Rena et al. 2017). The findings are also dose and treatment time dependent, with differences between acute and chronic administration. At molecular levels, metformin act via both AMP-activated protein kinase (AMPK)-dependent and AMPK-independent mechanisms. It inhibits mitochondrial respiration, but it seems to also inhibit mitochondrial glycerophosphate dehydrogenase which is a mechanism involving the lysosomes (Rena et al. 2017). The effects of metformin are due to affecting different signaling pathways, however the underlying mechanisms is still not fully understood (Lv and Guo 2020).

Figure 1.5: Chemical structure of metformin (PubChem 2021)

This is a 2D figure of the chemical structure of the drug metformin.

1.2.1 Metformin effect on cancer metabolism

The hypothesis that biguanides could be used for disease treatment was raised when phenformin was introduced and used to treat type 2 diabetes (Saraei et al. 2019). Phenformin was later shown to be toxic. Further studies raised the question if these types of drugs could be used for cancer treatment. Due to the toxicity of phenformin, metformin was the best candidate for cancer treatment trials. Recent studies and analysis have shown that metformin can reduce the proliferation of cancer cells and that the possibility of malignancies in a variety of cancer types also reduces (Saraei et al. 2019). These types include cancers such as breast, colon, prostate and pancreas. It has also been shown that metformin can be a promising candidate in combination treatment, along with radiotherapy metformin reduced tumor growth in cancers such as ovarian and melanoma. (Saraei et al. 2019)

One of the most intensively studied mitochondrial actions of metformin, which also is important for our study, is the inhibition of Complex I of the respiratory chain, see figure 1.6 (Rena et al. 2017). This suppresses ATP production from oxidative phosphorylation and affects the cells metabolism and triggers the cells adaptive energy-saving measures, involving downregulation of macromolecule synthesis. Mitochondrial inhibition also triggers the liver to compensate for the changes and lower the glucose release. This reduces the plasma glucose and insulin levels, as well as insulin-like growth factors and cytokines. These changes have shown to establish a less favorable environment for cancer cells and their proliferation. An important thing to notice is that these observations have not

only been seen in patients with diabetes, but it has also been observed in patients without diabetes (Rena et al. 2017).

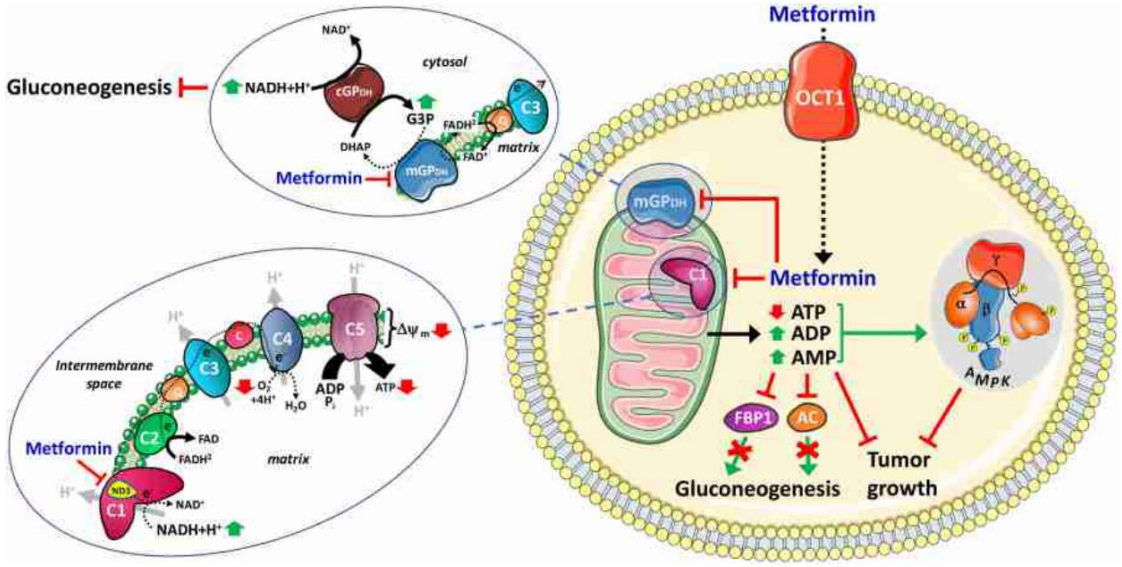

Figure 1.6: Metformin's effect on cancer cells (Vial et al. 2019)

This figure shows the mitochondria mechanisms of action of metformin. The drug is taken up by the cell, mostly through OCT1 in hepatocytes, and metformin's primary target is the mitochondria, it exerts specific inhibition on complex 1 of the respiratory chain through interaction with the ND3 core subunit and mitochondrial glycerophosphate dehydrogenase. When complex 1 is inhibit the NADH oxidation, proton pumping across the mitochondrial membrane and oxygen consumption rate decreases. This results in a lower gradient across the membrane and reduces proton-driven ATP synthesis from inorganic phosphate and ADP. When the mitochondrial glycerophosphate dehydrogenase is inhibited it modulates cytosolic and mitochondrial redox state which increases cytosolic NADH, adenylate cyclase and fructose-1,6-bisphosphate (Vial et al. 2019).

As mentioned earlier in this thesis, the exact mechanisms underlying the actions of metformin are still not clearly identified. The effect of the drug can vary due to the way it is used, if it is used alone or in a combination treatment with for example chemotherapeutic drugs, and the effect is also dose dependent (Chen et al. 2020). What we do know today is that a potent anticancer property of metformin is due to the activation of the LKB1-AMP-activated protein kinase (AMPK) signaling pathway. The drug increases the ratio of adenosine mono phosphate (AMP) to adenosine tri phosphate (ATP) by targeting complex I of the mitochondrial respiratory chain and thus activate the upstream kinase LKB1 that phosphorylates and activate AMPK. This activation can suppress mammalian target of rapamycin complex which are important in cell growth, proliferation and metabolism (Chen et al. 2020). Metformin can also inhibit complex I and mTORC1 activity in an AMPK-independent way, and metformin-induced activation of AMPK promotes PD-L1 phosphorylation which results in endoplasmic reticulum-associated PD-L1 protein degradation, and thus allows an cytotoxic T-lymphocyte mediated tumor cell death (Chen et al. 2020).

From the 2019 study by Saraei et al. there is listed a short brief of six effects of metformin based on various reputable published data and articles. See table 1.1 for effects (Saraei et al. 2019). Saraei et al also writes that metformin, due to all the benefits listed above, is an ideal candidate for cancer prevention, improvement in different treatments and preventing malignancy of tumors.

Table 1.1: the main effects of metformin on cancer cells (Saraei et al. 2019).

This table lists up the beneficial effects of metformin on cancer cells. All the information was found in the 2019 article by Saraei et al.

	The effects of metformin
1	Reduce the chance of cancer incidence
2	Reduce mortality of different cancers
3	When used in combination treatment with radiotherapy and chemotherapy, metformin increases the response
4	Reduces tumor malignity
5	Reduce likelihood for relapse
6	Reduces the damaging effects of androgen derivatives (ADT)

1.3 Database and Citavi

Metformin's effect on cancer cells have been researched for a long time, and there have been published numerous of scientific articles about the subject. This research holds valuable information for our research as well as for future studies. Extracting interesting data from different articles to make a database with important information was done by using a computer program named Citavi. 66 different articles were chosen, all of them having a common denominator being metformin, cancer cells metabolism and the "seahorse XF analyzer", which is an instrument used in measuring the oxygen consumption rate (OCR) and the extracellular acidification rate (ECAR) in live cells. As these measurements gives a good indication of how metformin effects the cancer cells metabolism, these results were of interest. Other parameter such as glucose concentration, metformin concentration, treatment time, viability, cell line and normalization method (of the seahorse XF analyzer) was also collected. Machine learning was used to interpret this data.

1.4 Seahorse XF

Seahorse XF analyzer is an instrument used in measuring the oxygen consumption rate (OCR) and the extracellular acidification rate (ECAR) in live cells. The OCR and ECAR gives information about the metabolism in the cells. The OCR gives a measure of mitochondrial function and is a marker of factors triggering the switch from healthy oxidative phosphorylation to aerobic glycolysis in cancer cells. The ECAR determines glycolysis by measuring the extracellular acidification rate of surrounding tissues, the excretion of lactic acid after its conversion from pyruvate (Agilent 2020).

1.4.1 Modulators in Seahorse XF analyzer

To find the OCR the seahorse XF analyzer adds modulators of respiration into the wells to find out the key parameters of mitochondrial function. The modulators are Oligomycin, Carbonyl cyanid-4 (trifluoromethoxy) phenylhydrazone (FCCP), Rotenone and Antimycin, see figure 1.7.

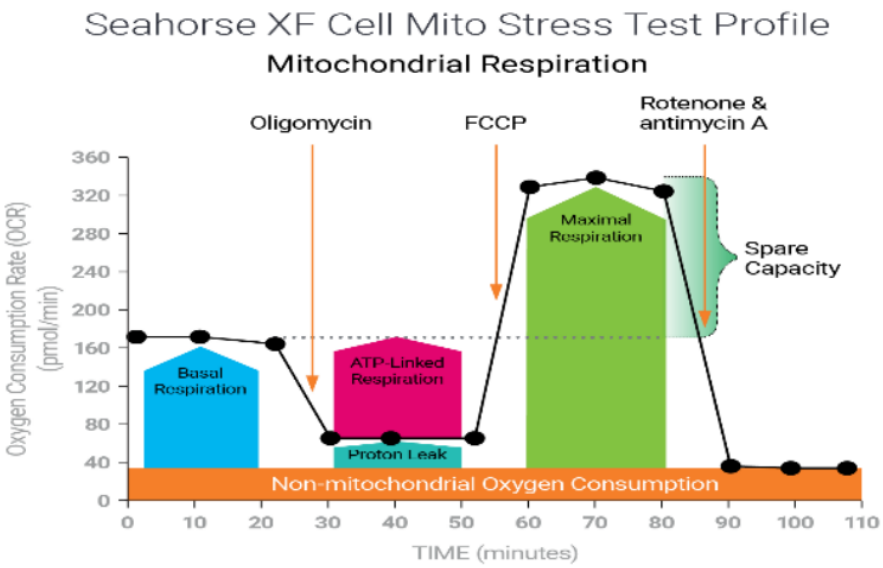

Figure 1.7: Seahorse XF cell mito stress test profile (Agilent 2020)

This figure shows the expected oxygen consumption rate in pmol/min in the mitochondrial respiration when the modulators oligomycin, FCCP, Rotenone and antimycin A are added (Agilent 2020).

The modulators who been adding are targeting the electron transport chain (ETC) in different ways. For example, Oligomycin inhibits complex 5 where ATP synthase is happening. FCCP are uncoupling the proton gradient generated by the mitochondrial membrane. The Rotenone are inhibiting the complex 1 by blocking the electron transfer from iron-sulfur centers in the complex (Heinz et al. 2017). Antimycin blocking the passage of electrons from cytochrome b to cytochrome c, thereby it inhibits the electron flow true complex 3 (Maria Ahmad et al. 2020), see picture 1.8 for an overview.

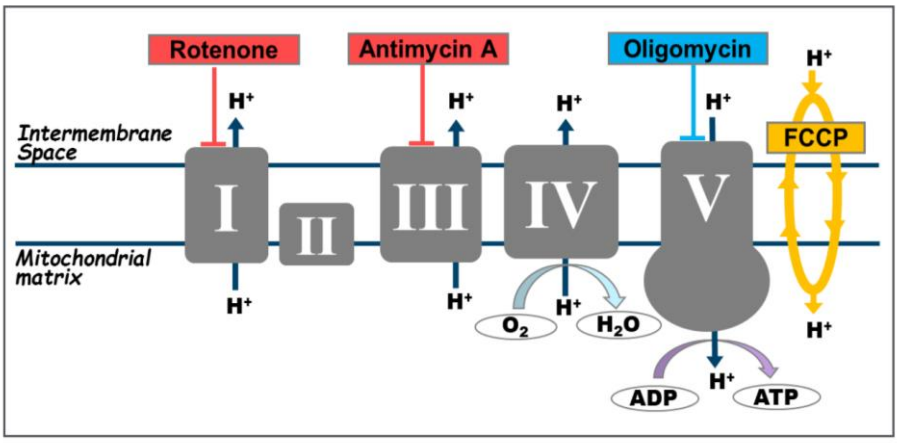

Figure 1.8: overview of the electron transport chain (Agilent 2020).

All modulators from the seahorse XF cell Mito stress test and all complexes in ETC are shown, the signs show were the modulators are active and inhibit the complexes.

1.5 Machine learning

Machine learning is an application of artificial intelligence with a primary aim of allowing the computer to learn automatically. It enables systems to learn and improve from previously experiences without being programmed (Expert.ai 2020). Machine learning holds a collection of data-analytical techniques with a purpose for building predictive models from multi-dimensional datasets. In medicine, machine learning is a growing field with many resources. It has the ability to deal with large and complex data which is often found within the medical field, and possibly is the future for biomedical research, personalized medicine, computer-aided diagnosis to significantly advanced global health care (Handelman et al. 2018). It is also becoming integral to modern biological research as it allows generation of models that learns from very large datasets and can make predictions based on these data. (Camacho et al. 2018).

As mentioned, machine learning gives the computers the ability to learn without first being programmed. This is done by introducing algorithms that ingest input data, use computer analysis for predicting values within an acceptable range of accuracy, identifying patterns in the data and learn for previously experiences. The idea of using machines to elucidate patterns and conclusions that are very difficult to reach by conventional statistical methods and that needs to be done manually by human operators is extremely relevant for the future. With machine learning this process is semiautomated, the computer is provided data and creates complex analytical models using learning framework to optimize the accuracy of prediction. (Handelman et al. 2018). Machine learning is not very different from conventional statistics, it is based on or adopts statistical underpinnings to how it works, but if much more efficient.

1.5.1 Machine learning basics

The data used in a machine-learning algorithm typically consists of parameters called “features” and “labels” across a set of samples. Features stands for the measurements across all samples and can be raw data or be transformed mathematically. Labels stands for the outcome that the models aim to predict, the outcome of the model. Machine learning algorithms may also interpret datasets lacking labels, see figure 1.9. The general workflow in machine learning is to first process the input data, then learn and/or train the model using a set of mathematical formulas and statistics, and at last use the model to predict a label of interest. The learning process consists of finding the optimal parameters for the model that translates the features from the data to accurate predictions of the labels. These parameters are estimated through a series of back and forth steps. Frist estimation, then the performance is evaluated, and errors are corrected, and new estimations are made and evaluated again. This is the process referred to as “training”, and it will repeat until the model performance can’t be further improved, which is assessed my error minimization. When the parameters are optimized the model can be used to predict outcomes of the model using new data (Camacho et al. 2018), see figure 1.9.

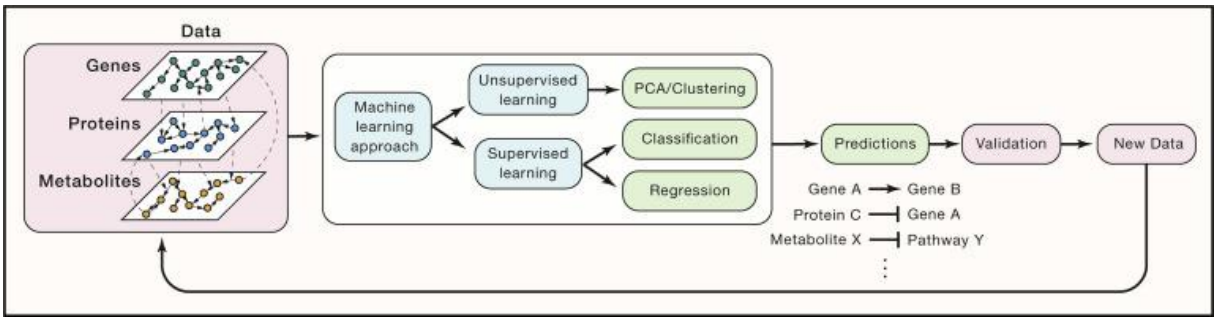

Figure 1.9: Machine-learning used to interpret and analyze datasets to build models

Example of how machine learning can be used to interpret data, here genes, proteins, and metabolites. The data consist of features that is measured over many samples and edges within networks. The machine-learning approach is selected based on properties of the data. If the data are unlabeled an unsupervised approach should be used, and if the data are labeled a supervised approach should be used and will generate a predictive model. After applying the most appropriate approach, the predictions made have to be validated. New data can be collected and used to refine the learned model and improve the performance (Camacho et al. 2018).

1.6 Muse® Count & Viability kit (200X)

To count and check the viability of the cells Muse® Count and viability kit (200X) were used. This machine finds viable cell count (cells/mL), total cell count (cell/mL) and precent viability of the sample. To do so the cell sample need to be mixed with Muse® Count & Viability reagent (200X) to get a DNA-binding dye in the reagent so it stains cells. Then it will be showing the result in a dotplot on the screen how much viable cells and non-viable cells it is. Another dye in the reagent are a membrane-permeant DNA staining dye that will stain all cells with a nucleus this will also be shown as a dotplot on the screen, see figure 1.10. This will discriminate cells from cells with a nucleus from non-nucleated cells and debri (Luminex Corporation 2020b).

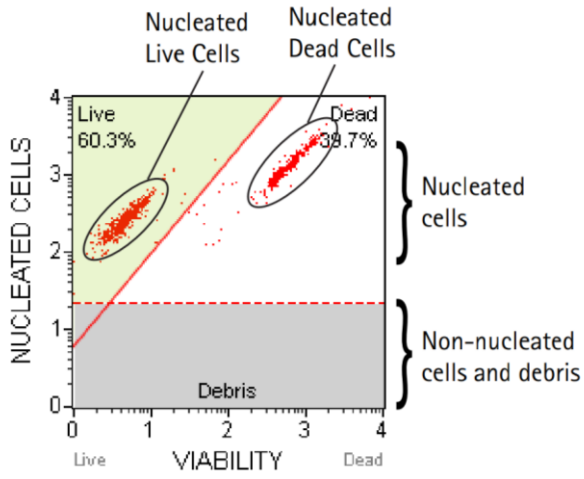

Figure 1.10: Illustration of the screen of the Muse count and viability machine (Luminex Corporation 2020a)

an illustration of how the result can look like on screen on the Muse Count & Viability machine (Luminex Corporation 2020a). The red dots illustrate nucleated cells, live (on the left) and dead (on the right). The green area shows the percentage of alive cells. The grey area represents cell debris (Luminex Corporation 2020b).

This system is a high-performance cell analyzing using a microcapillary technology. It has laser-based fluorescence detection and each cell event can evaluate up to three cellular parameters, see figure 1.11. (Luminex Corporation 2021).

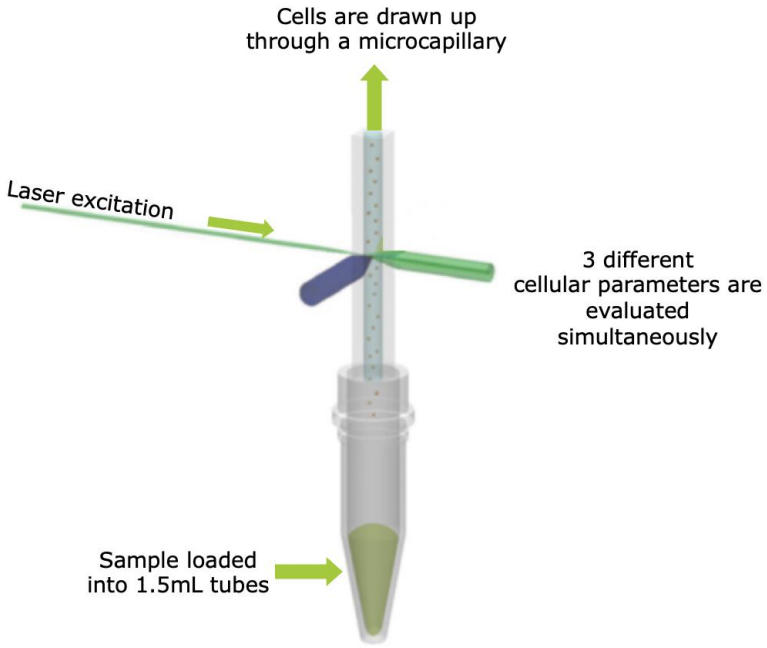

Figure 1.11: Illustration of how a cell samples viability is measured in the muse count and viability machine (Luminex Corporation 2020a)

The cell sample is loaded in a small tube and inserted into the machine. A green diode laser is used for excitation and each cell event can evaluate up to three cellular parameters cell size, detection in red color and detection in yellow color channels (Luminex Corporation 2021).

1.7 Aseptic cell culturing techniques

In labs, cells are grown “in vitro”, which means they are grown outside a living organism. Cancer cells are typically grown in flasks with growth media containing important ingredients for their survival (see section 2). The cells are kept in an incubator at appropriate temperature, human cells at 37°C to mimic body temperature. To keep the cells alive and comfortable, one must provide constant nutrients, so the medium in the flasks are aspirated regularly and new media is added. The cells are also passaged when they approach a certain confluency to avoid competition for nutrients and unwanted signaling between the cells. When working on cells in the lab aseptic techniques are used to keep the cells free from pathogens and avoid any contamination. The cell lab should be clean and kept as sterile as possible. All work should be done in a sterile fume hood. In this project a “LAF cabinet” was used. This is a sterile fume hood that has a laminar air flow that protect the cells from the user. This cabinet is not connected to a special ventilator that protects user from toxins, but when working on cells this is not needed, except when toxins are used as well. This kind of cabinet is crucial for working in a complete sterile environment. When working on cells one should also use gloves, protection clothing and face mask. Disinfection in the form of ethanol can be used to sterilize surfaces and instruments and is widely used in aseptic cell culturing.

1.7.1 Phosphate-Buffered Saline (PBS), Trypsin and media

Phosphate buffered saline (PBS) is used to wash the cells under passaging and is a non-toxic solution that prevents cells from shriveling or rupturing due to osmosis (Martin et al. 2006). In the culturing flasks cells adhere to the walls by proteins in the extracellular matrix. These proteins need to be digested by the enzyme trypsin before cell passage to break up adherent cells. Trypsin is a protease found in the digestive system of many vertebrates that hydrolyses proteins to polypeptides. The enzyme usually cuts the peptide chains in the carboxyl side in the amino acids' arginine or lysine. The proenzyme for trypsin is secreted from the pancreas and is activated in the duodenum. Trypsin is due to its efficacy and low cost used in numerous biotechnological processes (Store medisinske leksikon 2021). Under cell passaging the trypsin should not be let to digest for too long as this can result in damage to the cells. Therefore, inactivation of the enzyme after breaking up adherent cells is important. This can be done by fetal bovine serum which is a widely used serum in cell culture medium. In this experiment the serum was added to the medium used to contain cells in, that is described in the methods section. Fetal bovine serum contains anti-trypsin which is a substance that inactivates the trypsin and thus stop the digestion. L-glutamine and streptomycin was also added. L-glutamine is an amino acid supplement added to support growth in a cell culture and streptomycin is an antibiotic that protects the cell culture from bacteria.

1.8 Measuring cell viability

1.8.1 AlamarBlue

For over 50 years the reagent alamarBlue has been used for studies of cell viability and cytotoxicity in many different biological and environmental systems. The substance is widely used and generally its use has been applied to various aspects for monitoring cellular health, cell cycle, apoptosis, test compound toxicology in medicine, cytotoxicity and antimicrobial susceptibility testing (Rampersad 2012). In this project the alamarBlue was used to measure cell viability before and after metformin treatment.

The reagent can monitor the reducing environment of the living cell. Resazurin is the active reagent in alamarBlue and this is a water-soluble, non-toxic, stable in culture media and permeable through the cell membranes. This makes one able to continuous monitor the cells in the culture. Resazurin is a blue non-fluorescent dye that can be reduced to the pink colored, highly fluorescent resorufin, see figure 1.12. The reagent also acts as an intermediate electron acceptor in the electron transport chain without interfering with the normal functions of the chain. The indicator dye changes from the oxidized, non-fluorescent blue form to the reduced pink form when it accepts electrons. (Rampersad 2012)

Due to the changes of the resazurin from its oxidized to its reduced state, the reagent is very flexible when it comes to quantitative measurements as colorimetric and fluorometric readings, or qualitative as there is a visible change in color that indicates the presence of viable cells. The spectrometric absorbance can be taken at two wavelengths (570 nm and 600 nm or 540 nm and 630 nm). The fluorescence signals can be measured at excitation wavelength at 530-560 nm and an emission wavelength at 590 nm. (Rampersad 2012)

The culture media used in this kind of assay must be buffered as the optimal pH for the reagent is between 7.0 and 7.4. The optimal temperature for incubating the assay plate is 37°, and incubation should be done in the dark as alamarBlue is photosensitive. It is also important that the cell culture medium and all other reagents used in the assay does not interact with the assay chemistry. To avoid artifacts or false positive signals, the positive and negative controls should be empirically determined. The endpoint of the assay depends on which cell density was used. Cells in the assay

should be in exponential stage of growth and the medium should be synthetic and defined, but it have to allow sufficient growth so that inhibitory or stimulatory effects of compounds tested are not exaggerated or underestimated. (Rampersad 2012)

For this project the alamarBlue assay was very useful for the viability assay as it is easy to use and gives good results. The viability in two different cell lines, Panc-1 and MIA-Pa-Ca-2, was measured before and after metformin treatment. This was done by measuring the fluorescence signal at excitation wavelength at 540-590 nm using a SpectraMax® Paradigm® Multi-Mode Microplate reader, see figure 1.12.

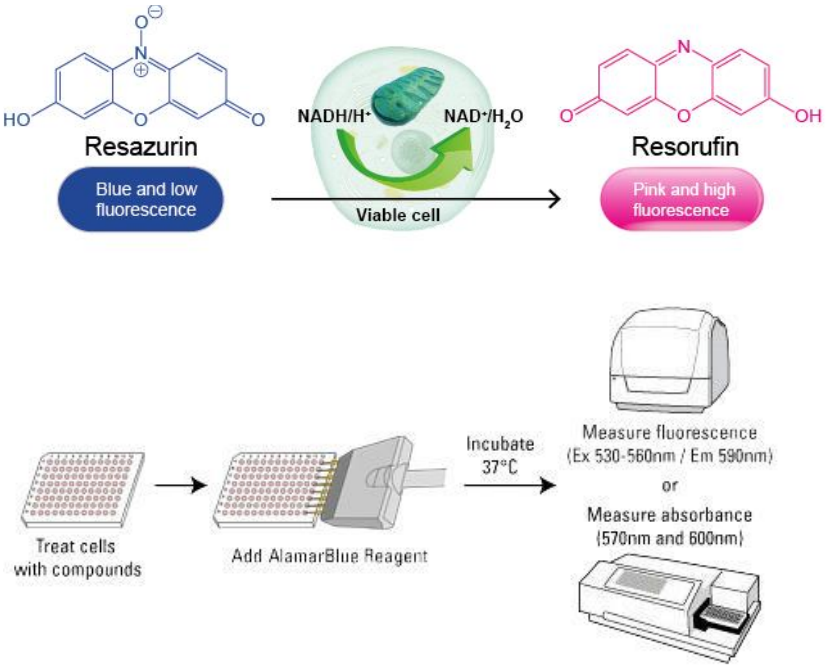

Figure 1.12: AlamarBlue resazurin reduction and equipment for measuring cell viability (ABP Biosciences 2021).

This figure shows the chemical composition of resazurin which is active reagent in alamarBlue. This reagent acts as an intermediate electron acceptor in the electron transport chain without interfering with the normal functions of the chain. When Resazurin accepts electrons, it is reduced to the pink, highly fluorescent resorufin that can be detected by a machine that can detect fluorescence and absorbance. Cell cultures are typically seeded out on a plate containing wells shown in the figure. This plate can be inserted to the machine directly and shows the results on an external screen (ABP Biosciences 2021).

1.8.2 CCK-8

The CCK-8 cell counting kit utilizes Dojindo's highly water-soulable tetrazolium salt and allows for very convenient assays. WST-8 [2-(2-methoxy-4-nitrophenyl)-3-(4-nitrophenyl)-5-(2,4- disulfophenyl)-2H-tetrazolium, monosodium salt] produces a formazan dye which is very water-soluble and that in the presence of an electron mediator is reduced, see figure 1.13. It is nonradioactive and allows sensitive colorimetric assays for determination viable cells in cell proliferation and cytotoxicity assays. As shown in figure 1.13, WST8 is reduced by dehydrogenases in the cells and gives the orange colored product formazan. This product is soluble in the tissue culture medium. The number of viable cells is directly proportional to the amount of the formazan dye generated by dehydrogenases in cells.

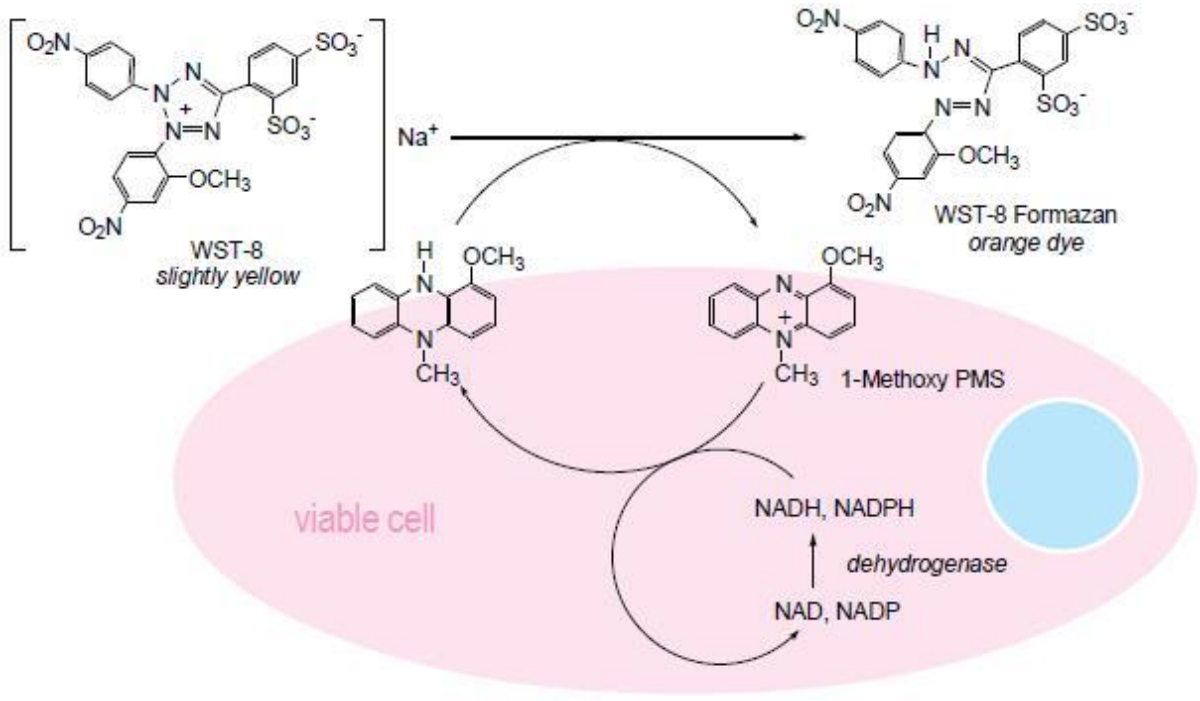

Figure 1.13: CCK-8 cell viability kit (Phd 2016)

The figure describes how the CCK-8 assay affect the cell and shows the chemical structure of the reagent before and after reduction. WST-8 (Dojindo's highly water-soluble tetrazolium salt is reduced to a yellow-color formazan dye by dehydrogenase activities in the cells. This dye is soluble in the tissue culture media. The number of viable cells is directly proportional to the amount of formazan dye (Phd 2016).

1.9 SpectraMax® Paradigm® Multi-mode Microplate reader

To measure cell viability a multi-mode microplate reader was used which can read fluorescence or absorbance across different wavelengths. These instruments are equipped with a Xenon flash lamp that can excite the fluorophore resorufin to be read at the appropriate emission wavelength. For the resazurin alamarBlue the machine read at 540 nm through the well and adjusted for background using the reference wavelength of 590 nm. Fluorescence can be explained by the absorption of light energy and its transformation into emission light. The light that is emitted has longer wavelength and is lower in energy than the light which is coming in, that is why the emission light always is higher wavelength (BMGLabtech.com 2021b).

When the machine measures the absorbance, it measures how much light is absorbed when the light goes through the sample. The machine quantifies the amount molecules in the solution which been absorbed of the light when the rest of the light hitting the detector on the other side (BMGLabtech.com 2021a). Formazan dye CCK-8 absorbance is read at wavelength 450 nm.

1.10 Aim for this project

In this collaboration bachelor thesis, we will focus on how understanding cancer cells metabolism can help us to develop better treatments for cancer patients. The understanding of how cancer cells reprogram and utilize glucose differently than normal cells is an important part of the development of new cancer treatments. Our main research is to study how the biguanide drug metformin can affect the metabolism in cancer cells, and therefore might be a future cancer treatment.

2. Materials and methods

2.1 Materials

All materials and chemicals used in this project were provided from associate professor Hanne Røland Hagland and her lab team. For clarity, everything is listed in tables, see table 2.1 and 2.2. Description of how the materials and chemicals was used will be in the coming section.

Table 2.1: Table of all the chemicals used in this project

This table lists chemicals with the corresponding producer/company and associated product number.

Product	Company	Product number
DMEM (Dulbecco's Modified Eagle's Media) without glucose, L-glutamine and sodium pyruvate	Corning	17-207-CV
Foetal bovine serum, heat inactivated, south American origin	Biowest	S181H-500
Penicillin: Streptomycin solution 6,0/10,0 g/L 100X	Biowest	L0022-100
Trypsin EDTA 1X	Corning	25-053-Cl
L-glutamine, 200mM	Corning	25-005-Cl
PBS tablet	ThermoFisher	189112-014
dH_2O		
MIA-Pa-Ca-2	ECACC General Collection	ECACC 85062806
Panc-1	ATCC	ATCC® CRL-1469
AlamarBlue	VWR	MFCD00005036
CCK-8	Tebu-bio	CK04-05
Metformin	Alfa Aesar	N27F021

Table 2.2: Materials used in this project

In this table the most important materials used in this project is listed.

Sterile bench	Microscope
Rack for tubes	96-wells plate
50 mL tube	T75 flasks
15 mL tube	Water bath
Eppendorf tube	Incubator
Automat pipette	Fridge
Pipettes for automat pipette	Freezer
Pipette controller	Aspiration-machine
Serological pipettes	Vortex mixer

2.2 Methods

2.2.1 Metformin seahorse XF dataset

In this project a dataset containing information on metformin effect on various cell lines was collected as mentions in section 1.3. The aim was to create a model that possible could help to predict the viability of the different cells when exposed to different concentrations and treatments times of metformin. This work was done in google collaborator and the coding library Pandas was used. The dataset was first uploaded here and then it was "cleaned", which means rows in the dataset lacking very much information was removed. A decision tree regression model was used, and validation of the model was done by splitting the dataset intro a training set and a testing set. The training set was used to fit the model and the testing set was used as validation data. The model made in this project was far from precise in predicting outcomes, but was more of a training exercise for understanding how machine learning works, and see the possibilities of this kind of work when done correctly by someone with good skills in this subject.

2.2.2 Media

The composition of complete cell culture media used is listed in table 2.3.

Table 2.3: All components to fix a DMEM complete media on a total volume of 562,22 mL, the result is a low glucose media (5 mM).

Components	**Amount in mL**
Dulbecco's Modified Eagle's Media, without glucose, L-glutamine and sodium pyruvate)	500
Foetal bovine serum, heat inactivated, South American origin	50
Penicillin; Streptomycin solution 6,0/10,0 g/L 100X	5
L-glutamine, 200 mM	5
Glucose, 2,4 mM	2,22

Foetal bovine serum is blood serum drawn from a bovine fetus and is one of the most used serum for growing cells in vitro in the lab, due to its high level of growth factors and low level of antibodies. This makes it usable for growing many different cell types. Penicillin is added to prevent bacterial growth in the cell culture, and glucose and glutamine are nutrients and amino acids the cells utilizes as an energy source and macromolecular synthesis respectively.

2.2.3 Media replacement

The cell media was changed every second day to ensure that the cells had enough nutrient. This was done in a sterile cabinet by aspirating the current medium and replacing it with 10 ml new DMEM complete medium pre-heated to 37°C.

2.2.4 Cell passaging

When the cell density in the culture flask (see figure 2.1) approach a certain confluency, they might start unwanted signaling that can interfere with experiments as well as stop growing and compete for space. The cells in this experiment was passaged routinely and the flasks the cells were contained in was changed once a week.

The cells were passaged when they approached 70-90% confluency. This was done in a sterile cabinet to avoid any contamination. All reagents and media used was heated to 37°C to match the temperature of the incubator the cells were contained in. The media in the flasks was aspirated and 2 ml PBS was added for cleaning. The PBS was aspirated carefully to not harm the cells, and 1 ml of trypsin was added. The trypsin was let to react for a couple of minutes. A microscope was used to closely watch the trypsin work and to determine when it was time to stop the digesting by adding 4 ml of complete DMEM media. The DMEM/trypsin mix was mixed using a pipette and then a volume of this was added to a new flask, or a certain volume was kept in the flask and the rest was removed, depending on the split ratio and if the cells needed a new flask. The flask was changed approximately 1 time each week to keep a clean environment for the cells. At last, DMEM complete media was added to have a total volume of 10 ml in the flask.

Figure 2.1: Cell culturing flask (Lifeline Cell Tech Team 2020).

This figure shows a cell culturing flask like the ones used in this project and a pipette that can be used to add the DMEM media.

2.2.5 Cell viability assay

The alamarBlue cell viability assays were done in a sterile cabinet to avoid any contamination. In the first step the medium in the flask was aspirated and the cells were rinsed with 2 ml PBS. After removing the PBS, 1 ml of trypsin was added and let to work, time depending on cell line, but approximately 1-2 minutes. The process was closely watched using a microscope. When the trypsin had broken up adherent cells, 4 ml of DMEM complete media was added and the culture was mixed carefully with a pipette. The trypsin/DMEM mix was transferred to a 15 ml tube to keep the cells from adhering. The cell density was measured using Muse cell viability kit and if the density was low, the tube was centrifuged so dead cells and cell debris could be removed. After centrifugation the cell will appear as a pellet in the bottom of the tube, and thus the media containing dead cells and debris could be removed and new medium was added. The volume of new medium was calculated to adjust the cell concentration to 500 000 cell/ml, making the calculation for the dilutions used in the assay easier. Five dilutions were made, containing 10 000, 15 000, 20 000, 25 000 and 30 000, respectively, see figure 2.2. Three parallels of each dilution (10 µl) were seeded out on a 96 well plate. 110 µl PBS was seeded out in the remaining empty wells, except for the four outermost corners. The plate was left to incubate for 48 hours in a cell incubator at 37°C.

After incubation, 10 µl of 484 µM resazurin at 37°C was added to each of the three parallels of each dilution, mixing with the pipette or shaking the plate to mix the reagent with the cell cultures. 110 µl of a positive control containing autoclaved medium and resazurin was seeded out in the four empty outermost corners for the alamarBlue assay. The plate was left to incubate for 4 hours in the cell incubator at 37°C. After incubation the plate was read by a SpectraMax® Paradigm® Multi-Mode Microplate reader to measure the fluorescence at 540-590 nm and hence the cell concentration.

Only alamarBlue assay was done for finding the cell density that showed the most accurate rising trend and should be used in the metformin experiment, both alamarBlue and CCK-8 assays was used in the metformin experiment. The CCK-8 assay is preformed the same way as the alamarBlue, except incubation time is two hours and one should measure the absorbance at 450 nm.

	1	2	3	4	5	6	7	8	9	10	11	12
A	Medium	PBS	PBS	PBS	PBS	PBS	PBS	PBS	PBS	PBS	PBS	Medium
B	PBS	0 cells	0 cells	0 cells	0 cells	0 cells	0 cells	0 cells	0 cells	0 cells	PBS	PBS
C	PBS	10 000 cells	10 000 cells	10 000 cells	10 000 cells	10 000 cells	10 000 cells	10 000 cells	10 000 cells	10 000 cells	PBS	PBS
D	PBS	15 000 cells	15 000 cells	15 000 cells	15 000 cells	15 000 cells	15 000 cells	15 000 cells	15 000 cells	15 000 cells	PBS	PBS
E	PBS	20 000 cells	20 000 cells	20 000 cells	20 000 cells	20 000 cells	20 000 cells	20 000 cells	20 000 cells	20 000 cells	PBS	PBS
F	PBS	25 000 cells	25 000 cells	25 000 cells	25 000 cells	25 000 cells	25 000 cells	25 000 cells	25 000 cells	25 000 cells	PBS	PBS
G	PBS	30 000 cells	30 000 cells	30 000 cells	30 000 cells	30 000 cells	30 000 cells	30 000 cells	30 000 cells	30 000 cells	PBS	PBS
H	Medium	PBS	PBS	PBS	PBS	PBS	PBS	PBS	PBS	PBS	PBS	Medium

HCT 116 Mia-Pa-Ca-2 PANC1

Figure 2.2: Plate layout alamarBlue cell viability assay

This figure shows the locations of the different concentrations of cell suspensions of three cell lines, only Mia-Pa-Ca-2 and Panc-1 was used in this experiment. It also shows the four positive controls (it says medium not positive control, as the medium was seeded out first and then replaced with positive control) in the outermost corners and the rest filled with PBS.

2.2.6 Muse® Count & Viability kit (200X)

Before start 0.5 mL of cell sample were poured into an ependorftube. In a 1.5-mL microcentrifuge tube 10 µL of cell sample who were mixed by pipetting and 190 µL Muse® Count & Viability reagent were add, the dilutions factor was 20. The tube with both components were mixed well by vortexing so no purple color was left. The tube with sample was incubated in room temperature for 5 minutes before loading it into the instrument. All steps were shown at the screen on the instrument and the result were noted

2.3 Metformin trial

2.3.1 Calculations

The trial start with the calculations, all volumes were measured for three cell-lines whereas two were used in this trial. Metformin comes in powder form and was mixed with MQ-water to make the 250 mM metformin stock.

700 µL Metformin stock per cell-line:

$$700 \times 3 = 2100\ \mu L\ = 2{,}1\ mL$$

Two tests → $2{,}1 \times 2 = 4{,}2\ mL$

Metformin in grams:

$$\boldsymbol{n = C \times V}$$

$$C = 250mM\ = 0{,}250M$$

$$V = 4{,}2\ mL = 0{,}0042\ L$$

$$n = 0{,}250 \times 0{,}0042 = 0{,}00105\ mol$$

$$\boldsymbol{m = n \times M}$$

$$n = 0{,}00105\ mol$$

$$M = 129{,}16\ g/mol$$

$$m = 0{,}00105 \times 129{,}16 = 0{,}135618\ gram = 135{,}618\ mg$$

250 mM metformin in volume:

$$\boldsymbol{C_1 \times V_1 = C_2 \times V_2}$$

$$C_1 = 250\ mM$$

$$V_1 = X$$

$$C_2 = 1{,}5\ or\ 10\ mM$$

$$V_2 = 4200\ \mu L$$

$$\boldsymbol{V_1 = \frac{C_2 \times V_2}{C_1}}$$

$$V_{10mM} = \frac{10mM \times 4200\ \mu L}{250mM} = 168\ \mu L$$

$$V_{5mM} = \frac{5mM \times 4200\ \mu L}{250mM} = 84\ \mu L$$

$$V_{1mM} = \frac{1mM \times 4200\ \mu L}{250mM} = 16{,}8\ \mu L \approx 20\ \mu L$$

Table 2.3: Calculated values for making metformin/DMEM media solutions

Metformin and media volumes for right concentrations, total volume 4200 µL.

	Metformin in µL	**Complete media in µL**
10 mM	168	4032
5 mM	84	4116
1 mM	20	4180

2.3.2 Preparation of plate

The cells were measured using the MUSE count and viability kit (200X): depends on how much cells/mL it is, dilution after table 2.4 is needed.

Table 2.4: Table of correct volumes of muse reagent contra cell suspension for measuring cell viability

This table was collected from the website/protocol? of company that provides the muse count and viability machine and reagents. It shows what volume of the muse reagent to use for different concentrations of cell suspensions and what dilution factor this corresponds to (Luminex Corporation 2020a)

Conc. Of orginal cell suspension	**Dilution factor**	**Cell suspension volume**	**Count and viability volume**
1×10^5 *to* 1×10^6 $Cells/mL$	10	25 µL	225 µL
1×10^6 *to* 1×10^7 $Cells/mL$	20	10 µL	190 µL
$> 1 \times 10^7$ $Cells/mL$	40	10 µL	390 µL

If the density in the sample is low, it is possible to centrifuge the tube. It helps to remove some of the dead cells and debris, also it decreases trypsin in the sample. After centrifuging most of the viable cells will appear as a pellet in the bottom of the tube, all media over this pellet was aspirated off and new fresh media was added before the pellet was resuspended.

Total viable cells in original sample = X, to adjust the cell concentration to 500 000 cell/mL, Y = volume of medium to add in the tube:

$$\frac{X}{500\,000} = Y\ mL$$

When the tube contains 500 000 cells/mL, 840 µL was added to a new tube and 3360 µL Complete media was added (total 4200 µL). The final concentration was 10 000 cells/100µL.
100 µL will be seeded out in the colored wells on the plate, see figure 2.3.

	1	2	3	4	5	6	7	8	9	10	11	12
A	Pos. Control						Pos. control					
B		Control	Control MQ	1mM Met	5mM Met	10mM Met						
C		Control	Control MQ	1mM Met	5mM Met	10mM Met						
D		Control	Control MQ	1mM Met	5mM Met	10mM Met						
E		Control	Control MQ	1mM Met	5mM Met	10mM Met						
F		Control	Control MQ	1mM Met	5mM Met	10mM Met						
G		Control	Control MQ	1mM Met	5mM Met	10mM Met						
H	Pos. Control						Pos. control					

Figure2.3: Figure of the plate layout of the 96-wells plate used in metformin experiment

This figure shows the placement of the controls and the three different metformin treatments. 10 000 cells of the Panc-1 and MIA-Pa-Ca-2 cell lines (1 cell liner per plate) was seeded out in each of the colored wells in the figure. After letting the cells adhere, medium was aspirated and the different treatments of control with medium, control with media and MQ water and three different metformin concentrations in medium (1 mM, 5 mM and 10 mM) was added. The plate was incubated for 24 or 48 hours. In the blue wells alamarBlue reagent was added and in the pink wells CCK-8 reagent was added before incubating and measuring fluorescence and absorbance.

Controls

Control with distillated water was made as the highest concentration of metformin, table 2.3 showed 168 µL of distillated water and 4032 µL Complete media was mixed and added in the wells. Figure 2.3 shows place in plate.

Control was the cells who only been exposed to media, positive controls was autoclaved resazurin and in the empty cells around the occupied wells were filled with PBS. Figure 2.3 shows place in plate.

Stock concentration with metformin

A tube with metformin and distillated water was made. Metformin was weighed to 135,6 mg and 4,2 mL distillated water was added, the final concentration was 250mM.

From the stock with 250mM metformin three new tubes was diluted to a concentration of 1, 5 and 10 mM, total volume was 4200 µL in each tube, see figure 2.4.

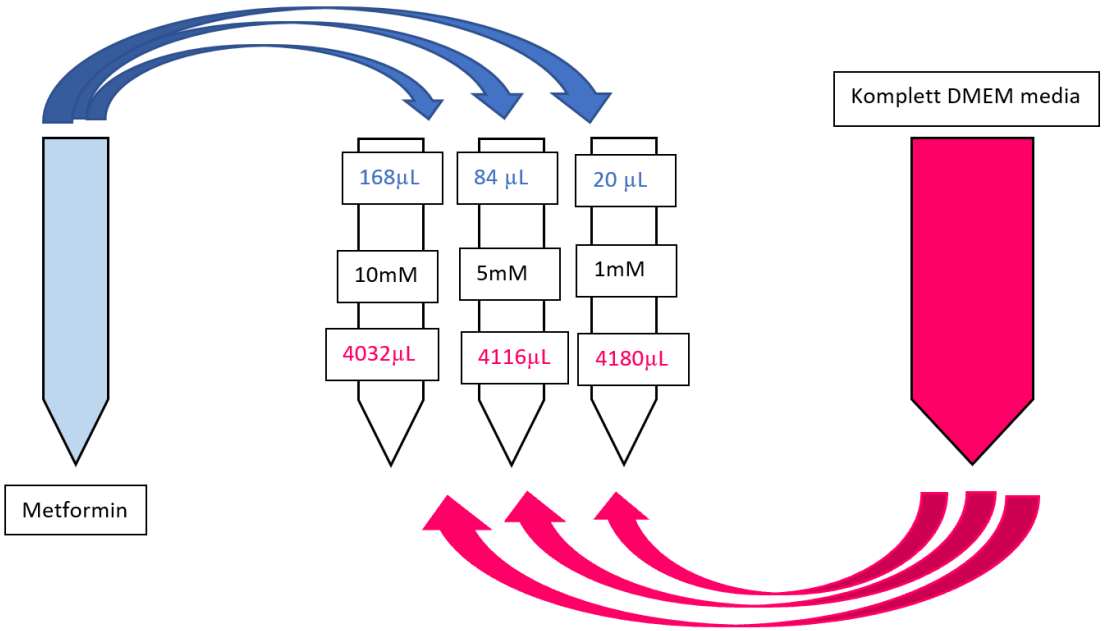

Figure 2.4: Illustration of making dilutions of different metformin concentrations in DMEM media

This figure shows an overview of how to dilute 250 mM metformin into 1 mM, 5 mM and 10 mM concentrations in DMEM media.

Second day was all media aspirated and 100 µL new fresh media with metformin was added. Media with metformin solution was made the day before.

Third (24 hours plate) and fourth day (48 hours plate) was all media with metformin aspirated and new fresh media was added. Four hours before the plate was read in SpectraMax Paradigm Multi-mode microplate reader the blue wells in figure 2 was aspirated and 100 µL new fresh media mixed with 10 µL alamarBlue was added and then incubated.

2,5 hours before the plate was read the pink wells in figure 2 was aspirated and 100 µL fresh media mixed with 10 µL CCK-8 was added before incubating until the reading of plate.

When the plate was read it was done two times, first the alamarBlue wells was read at fluorescence at 590 nm, and after the CCK-8 wells was read at absorbance at 450 nm.

3. Result

3.1 Pancreatic cancer cell growth and optimal seeding density

The pancreatic cell lines in this experiment were MIA-Pa-Ca-2 (Figure 3.1) and Panc-1 (Figure 3.2). Both cell lines survived, proliferated and was free for any contamination when contained in the DMEM complete low glucose media throughout the experiments. The routinely passaging when approaching approximately 70% confluency worked well for both cell lines. We found that the Panc-1 cell line grew slower than MIA-Pa-Ca-2 and was therefore passaged at a lower ratio to make sure the density of cells was kept at the number needed to complete our experiments.

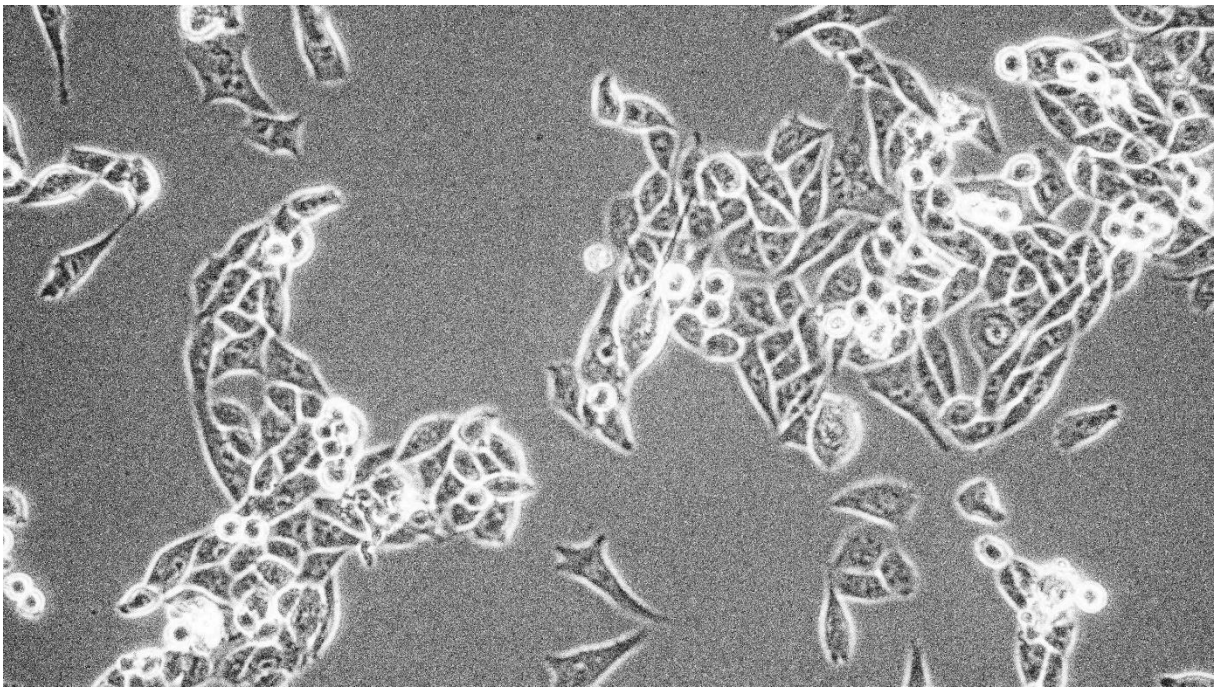

Figure 3.1: MIA-Pa-Ca-2

Microscope picture of the MIA-Pa-Ca cell line. The morphological features of MIA-Pa-Ca-2 are a longer form with sharp corners

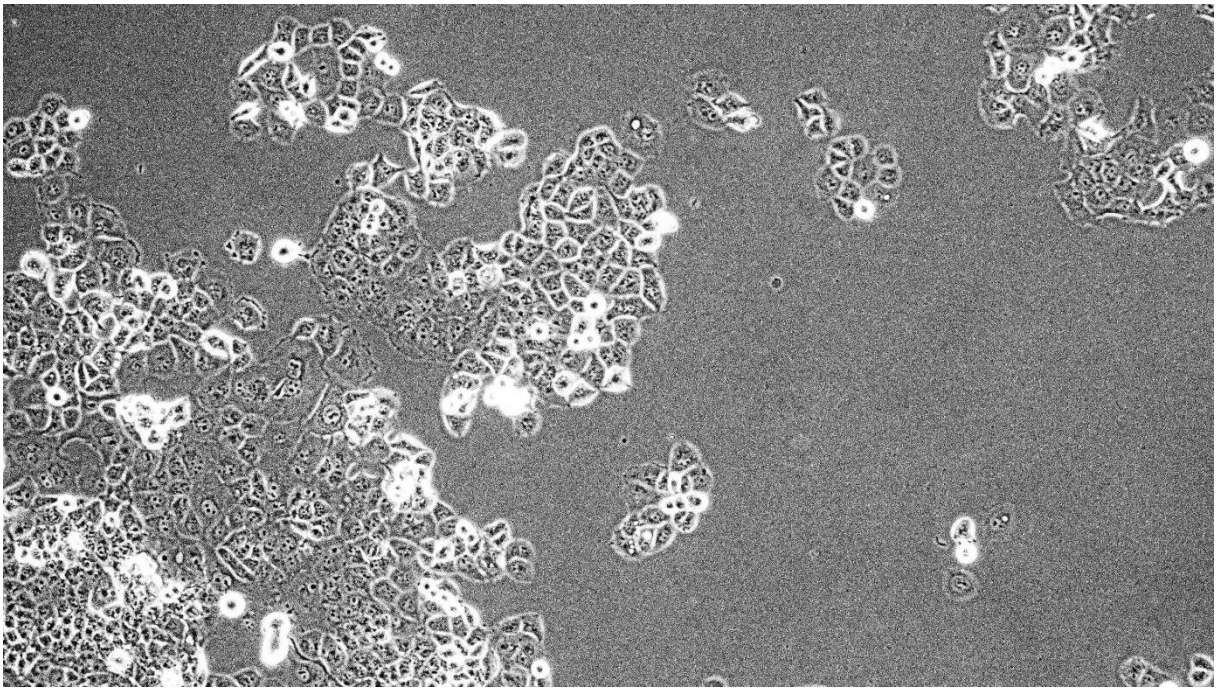

Figure 3.2: Panc-1

Microscope picture of the Panc-1 cell line. The morphological features of Panc-1 were more oval and smaller than MIA-Pa-Ca-2.

To find the optimal seeding density to be used for drug treatment experiments we seeded different cell numbers in 96 well cell culture plates to be read using the alamarBlue viability assay. The first cell seeding results are shown in figure 3.3. Here we see that there is an increase in fluorescence according to increasing cell density in both MIA-Pa-Ca-2 and Panc-1.

In this experiment it seemed like the MIA-Pa-Ca-2 reached a plateau with regards to the fluorescence at 10 000 cells/well that did not further increase in the higher cell numbers. The same trend was not seen for Panc-1 as there was a slight increase in fluorescence from 10 000 cells/well to 20 000 cells/well. The standard deviation for the Panc-1 cell line showed that there was low variation in cell density in the three well parallels. The wells that should contain 25 000 and 30 000 cell/well was empty on the plate containing Panc-1 cells as there were not enough cells for the experiment.

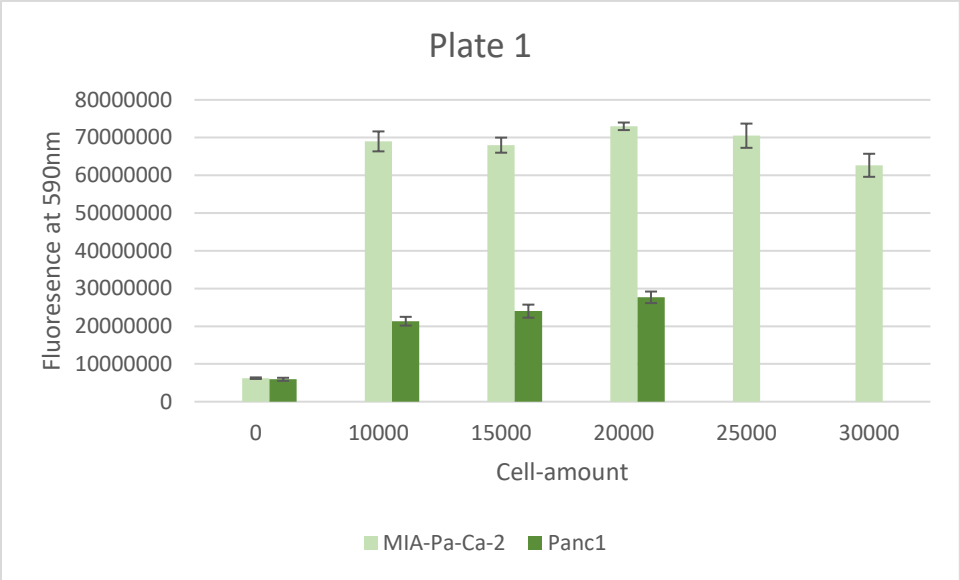

Figure 3.3: AlamarBlue cell viability assay results week 1

Results from alamarBlue cell viability assays done on the cell lines Panc-1 and MIA-Pa-Ca-2. Both cell lines were seeded out on a 96-well plate in the densities 10 000, 15 000, 20 000, 25 000 and 30 000 cells/well. The cells were let to adhere and after this 10 µl of the reagent was added. The reagent was let to work for 4 hours. Fluorescence was measured at 540-590 nm.

The second assay showed slightly different results from the first experiment where there was an increase in fluorescence according to cell density for the cell line MIA-Pa-Ca-2, see figure 3.4. The cell density rose evenly from the wells containing 10 000 cell/ well to the wells containing 30 000 cells/well. In this experiment the Panc-1 fluorescence did not change much ranging from 10 000 cells/well to the 30 000 cells/well. The standard deviation showed that the cell density of the parallels varies more for the Panc-1 cell line than the MIA-Pa-Ca-2 but was relatively low for both cell lines.

Figure 3.4: AlamarBlue cell viability assay results week 2

Results from alamarBlue cell viability assays done on the cell lines Panc-1 and MIA-Pa-Ca-2. Cells were seeded out on a 96-well plate in the densities 10 000, 15 000, 20 000, 25 000 and 30 000 cells/well. The cells were let to adhere and after this 10 µl of the reagent was added. The reagent was let to work for 4 hours. Fluorescence was measured at 540-590 nm.

The final cell seeding experiment was performed on MIA-Pa-Ca-2 cell line alone as there were issues with the Panc-1 cell seeding and these wells were not used for further assay analysis.

This third assay confirmed that MIA-Pa-Ca-2 shows an increase in fluorescence according to cell density up to 30 000 cells/well, see figure 3.5.

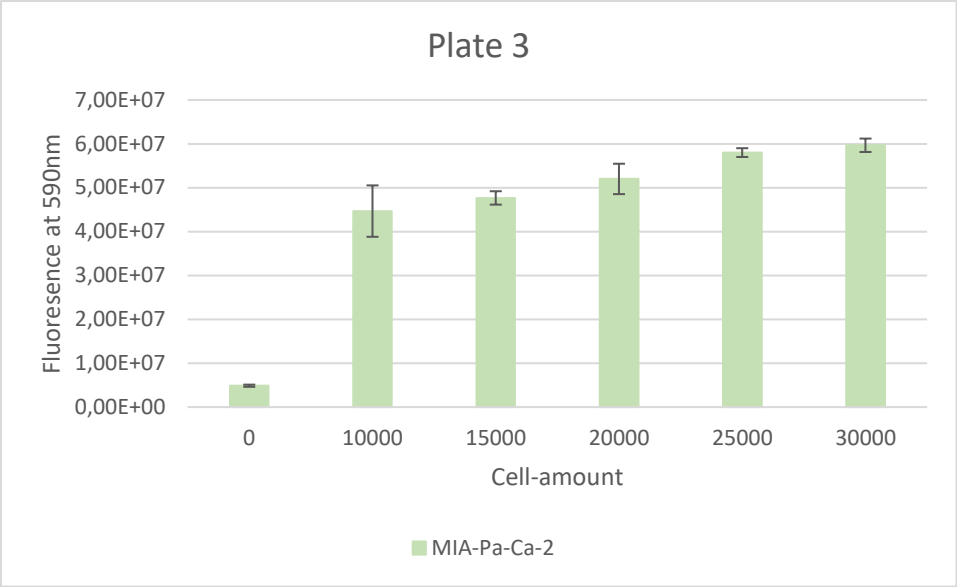

Figure 3.5: AlamarBlue cell viability assay results week 3

Results from alamarBlue cell viability assays done on the cell line MIA-Pa-Ca-2. The cells were seeded out on a 96-well plate in the densities 10 000, 15 000, 20 000, 25 000 and 30 000 cells/well. The cells were let to adhere and after this 10 µl of the reagent was added. The reagent was let to work for 4 hours. Fluorescence was measured at 540-590 nm.

As we wanted to be within the sensitivity of the assay when performing our drug screening, we chose to use 10 000 cells/well for both cell lines in the continuing experiments.

3.2 Metformin treatment in pancreatic cancer cell lines

3.2.1 MIA-Pa-Ca-2

All results were normalized to control containing DMEM media only.

AlamarBlue and CCK-8 assay after metformin treatment, 24 hours plate MIA-Pa-Ca-2

On the 24 hours plate for MIA-Pa-Ca-2 shows from week 1 and week 2 a similar pattern on both fluorescence at 590 nm with alamarBlue and on absorbance at 450 nm with CCK-8. This actively means that it is not much derivation on the two plates consider the seeding of cells in wells and the adding of alamarBlue and CCK-8. See figure 3.6. In week 2 CCK-8 assay there is a small increase in viability from the water control to the 1 mM metformin treatment. The standard deviation for both weeks is low, meaning that there is consistency in our set up of the plates.

From the graphs it shows a small decrease in cells alive when metformin concentration increase.

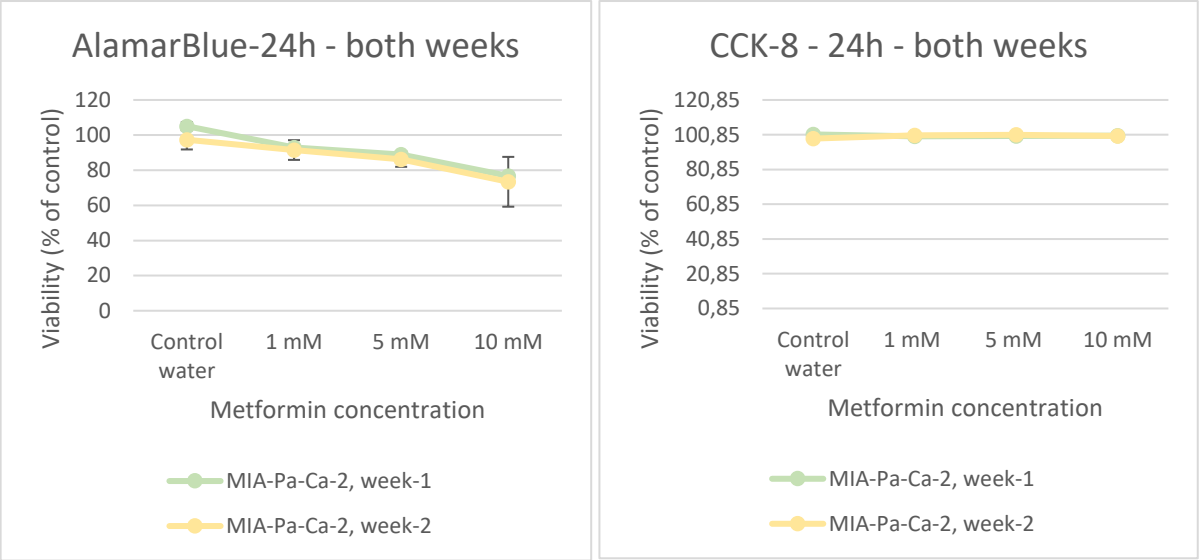

Figure 3.6: Results from cell viability assay of the MIA-Pa-Ca-2 cell line after 24 hours of metformin treatment

This figure shows two cell viability assays done on the MIA-Pa-Ca-2 cell line after treatment with 1 mM, 5 mM and 10 mM metformin for 24 hours. The experiment was done twice, week 1 and week 2. For each week two 96-wells plates were prepared by seeding out 10 000 cell/ well of the MIA-Pa-Ca-2 cell line. There was prepared one control with DMEM media only, and one with DMEM media and MQ-water. For the alamarBlue assay positive control was added. Six parallels on each plate were treated with the different metformin concentration. Half of the parallels were treated with alamarBlue reagent, and the other three were treated with the CCK-8 cell viability reagent. The figure to the left shows the fluorescence measured at 540-590 nm after addition of alamarBlue reagent. The figure on the right shows the absorbance measured at 450 nm after addition of the CCK-8 reagent. The results were normalized to the DMEM only control.

AlamarBlue assay after metformin treatment, 48 hours plate MIA-Pa-Ca-2

In the 48 hours metformin treatment there is a sharp decline in viability at the 5mM metformin concentration for MIA-Pa-Ca-2 which further decreases at the 10mM metformin concentration, see figure 3.7. Week 1 shows a larger decrease in alive cells when metformin concentration gets higher than week 2, especially after 1 mM.

CCK-8 assay after metformin treatment 48 hours plate MIA-Pa-Ca-2

Water control and 1 mM for both weeks are following the same curve, then it's a big jump from 1 mM to 5 mM and it is a big difference between week 1 and 2. From week 1 the metformin concentration from 5 mM to 10 mM have almost the same viability of cells, but for week 2 there is a large decrease.

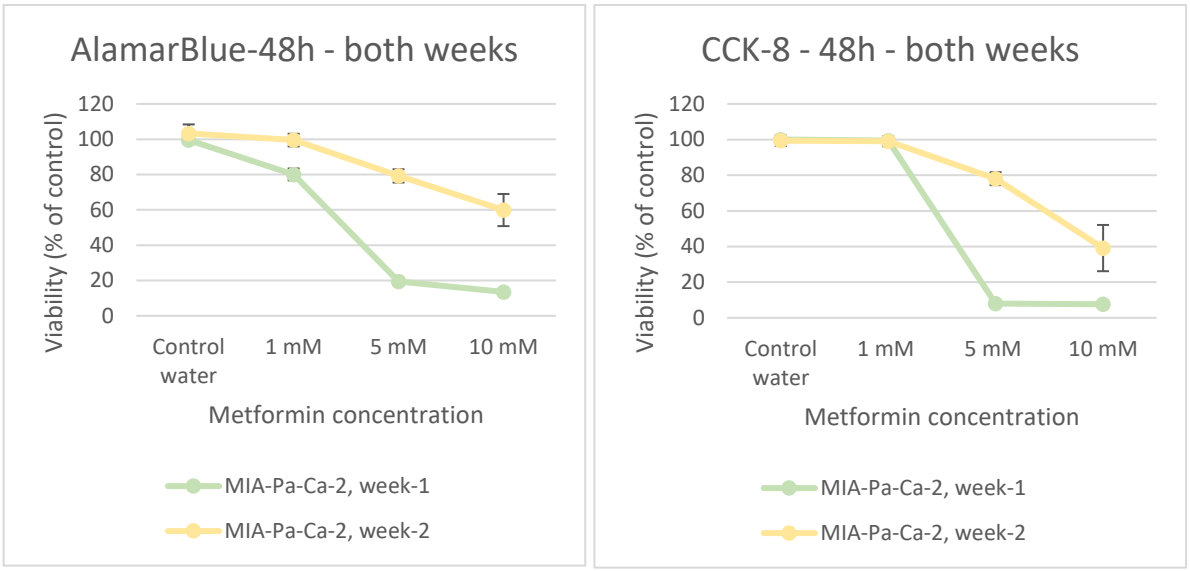

Figure 3.7: Results from cell viability assay of the MIA-Pa-Ca-2 cell line after 48 hours of metformin treatment

This figure shows two cell viability assays done on the MIA-Pa-Ca-2 cell line after treatment with 1 mM, 5 mM and 10 mM metformin for 48 hours normalized to control containing DMEM medium only. The experiment was done twice, week 1 and week 2. For each week two 96-wells plates were prepared by seeding out 10 000 cell/ well of the MIA-Pa-Ca-2 cell line. There was prepared one control with DMEM media only and one with DMEM media and MQ-water. Positive control was added for the alamarBlue assay. Six parallels on each plate were treated with the different metformin concentration. Half of the parallels were treated with alamarBlue reagent, and the other three were treated with the CCK-8 cell viability reagent. The figure to the left shows the fluorescence measured at 540-590 nm after addition of alamarBlue reagent. The figure on the right shows the absorbance measured at 450 nm after addition of the CCK-8 reagent.

A picture was taken at the wells with some deviation after the plate was read, see figure 3.8 and 3.9. The pictures show a large bubble in the left corner which can act to obscure the reading, see figure 3.8. The other wells had a more evenly spread in the cells, as shown in figure 3.9 are more compact on top of each other in some places.

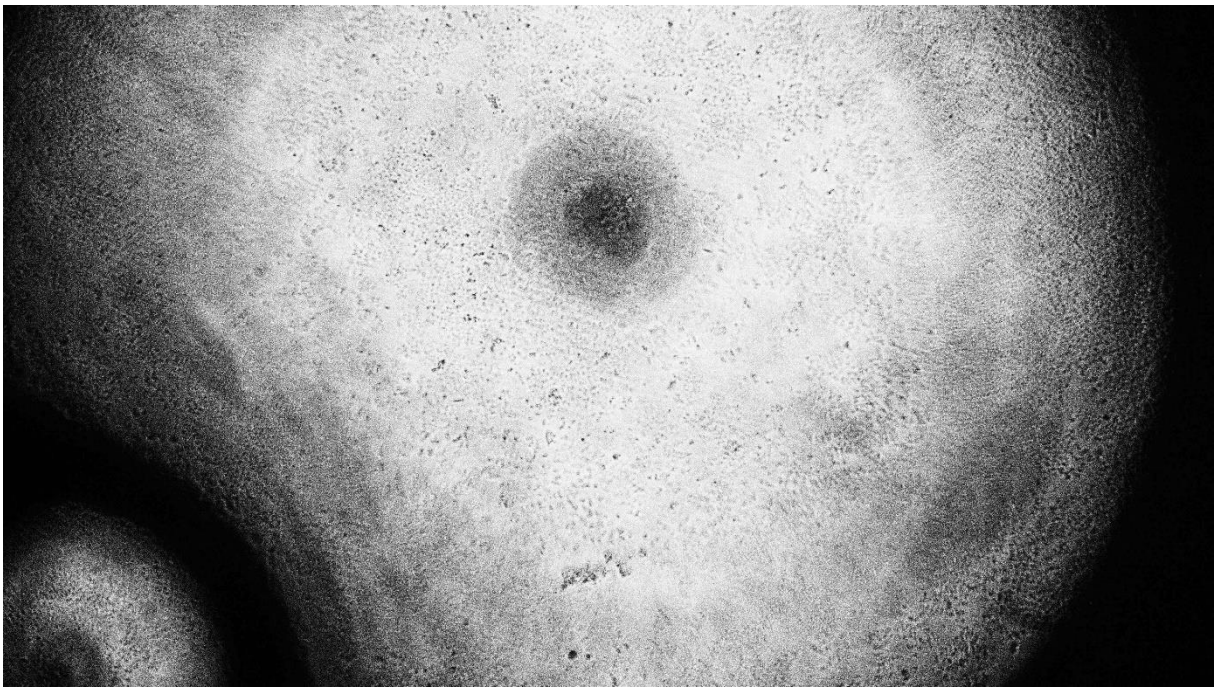

Figure 3.8: Microscope picture of MIA-Pa-Ca-2 in a 96 wells plate

This figure shows a picture of one of the wells who had a deviation who was visible for the eye to see. In the left down corner, it shows a big bubble who can be the result of some deviation in the measurement and made a bigger standard deviation in the graphs.

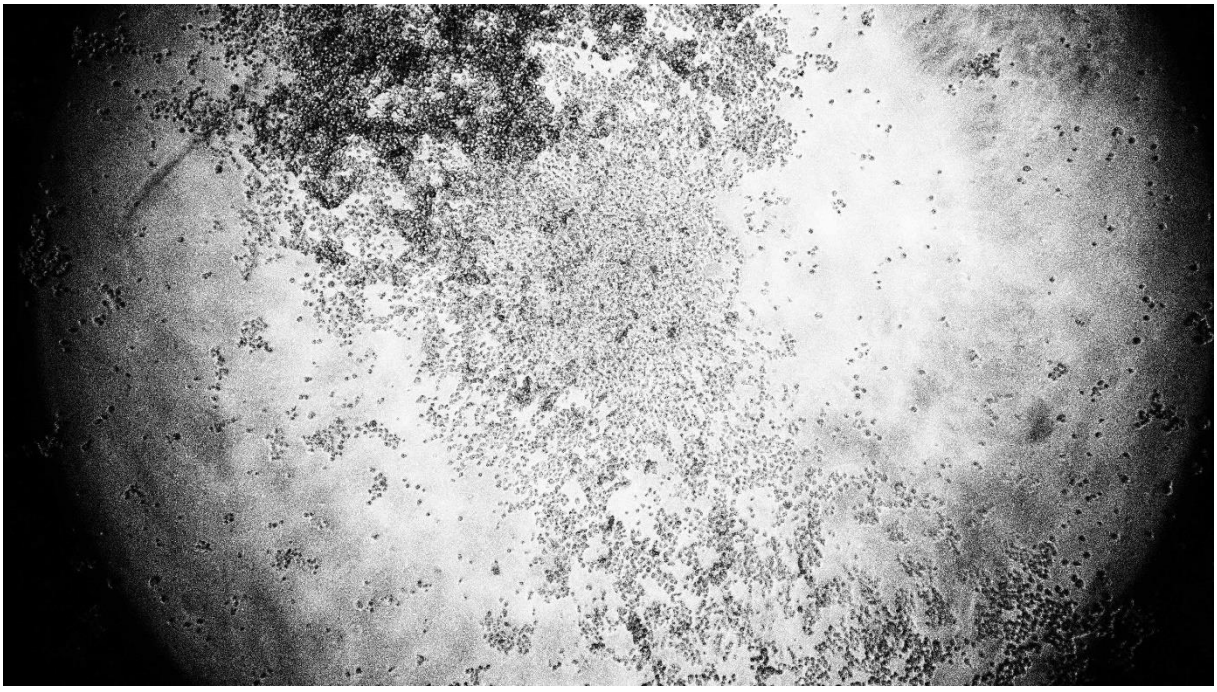

Figure 3.9: Microscope picture of MIA-Pa-Ca-2 cell line on a 96 wells plate

This figure shows a visible deviation for the eye to see with the lighter color in this well. As shown the cells look more compact and in a larger colony in the upper part of the well, this can be the result of the deviation in the measurement and made a bigger standard deviation in the graphs.

To sum up everything that has been stated so far, this research shows the metformin have an impact on MIA-Pa-Ca-2 cells, when the metformin concentration increases up to 10 mM the cells alive are decreased.

3.2.2 Panc-1 cells

All results were normalized to control. The week 1 plate lacked control with DMEM media only and was therefore normalized to the control containing DMEM medium and MQ-water.

Alamarblue assay after metformin treatment, 24 hours plate Panc-1

The first week the results showed a decrease in viability from the control with MQ-water to the first metformin treatment (1 mM). From 1 mM to 5 mM the viability decreased, but from 5 mM to 10 mM it increased as shown in figure 3.10. The second week the viability increased when treated with 1 mM compared to the MQ-water control, but then decreased continuously from 1 mM to 10 mM metformin treatment. The standard deviations were very high in the first assay compared to the second one.

CCK-8 assay after metformin treatment, 24 hours plate Panc-1

In this assay the viability decreased from the MQ-water controls to the first metformin treatment of 1 mM in both weeks. The first assay done (week 1) had a decrease in viability from 1 mM to 5 mM, but likewise the alamarBlue assay, the viability increased from the wells treated with 5 mM to 10 mM. The second week the viability decreased continuously from 1 mM treatment to 10 mM treatment. The standard deviations were higher for the second week assay compared to the first week, especially in the three parallels containing 5 mM metformin, see figure 3.10.

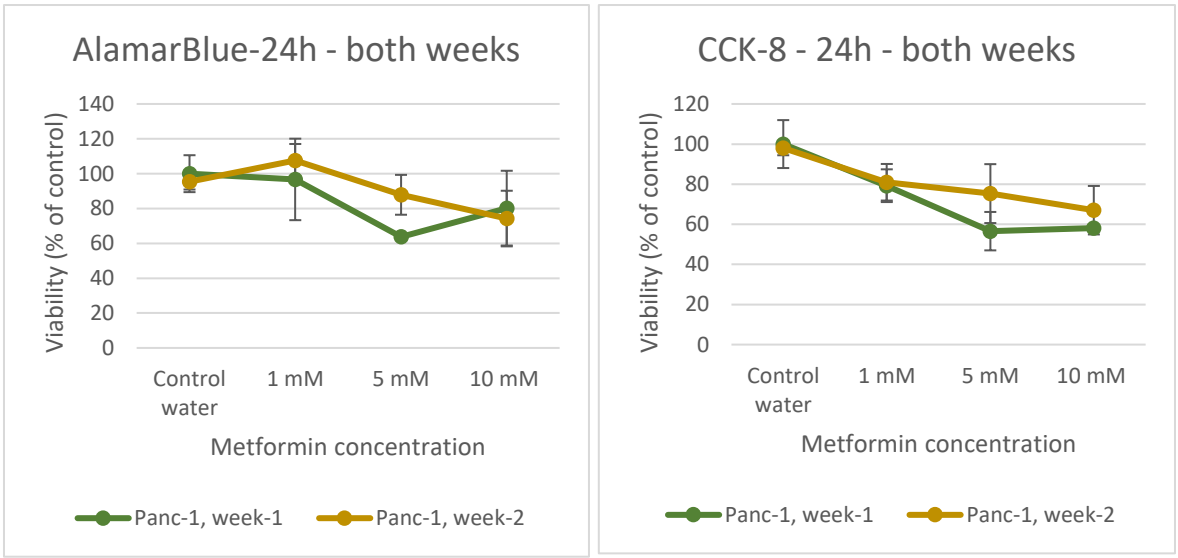

Figure 3.10: Results from cell viability assays of the Panc-1 cell line after 24 hours of metformin treatment

This figure shows two cell viability assays done on the Panc-1 cell line after treatment with 1 mM, 5 mM and 10 mM metformin for 24 hours. The experiment was done twice, week 1 and week 2. For each week two 96-wells plates were prepared by seeding out 10 000 cell/ well of the Panc-1 cell line. There was prepared one control with DMEM media only (missing on week 1 plate due to errors), and one with DMEM media and MQ-water. For the alamarBlue assay positive control was added. Six parallels on each plate were treated with the different metformin concentration. Half of the parallels were treated with alamarBlue reagent, and the other three were treated with the CCK-8 cell viability reagent. The figure to the left shows the fluorescence measured at 540-590 nm after addition of alamarBlue reagent. The figure on the right shows the absorbance measured at 450 nm after addition of the CCK-8 reagent. The results for week 1 are normalized to control with MQ-water, and the week 2 results are normalized to the DMEM media only control.

AlamarBlue assay after metformin treatment, 48 hours plate Panc-1

The first assay done (week 1) showed a small decrease in cell viability from the control with MQ-water to the first metformin treatment of 1 mM. It had the highest decrease in cell viability from 1 mM to 5 mM metformin treatment, and from 5 mM to the 10 mM the cell viability was almost constant, see figure 3.11. The second assay done also had a decrease in viability from MQ-water control to the 1 mM metformin treatment. This assay also had the highest decrease in viability going from 1 mM treatment to 5 mM treatment, see figure 3.11. The cell viability decrease flattens out and is almost constant from 5 mM to 10 mM of metformin treatment, like the first week. The standard deviations were very high, especially for the week 2 assay and shows that there was a lot of variation between the three parallels.

CCK-8 assay after metformin treatment 48 hours plate Panc-1

The first assay done (week 1) had a large increase in cell viability in the control parallels with media and MQ-water to the first metformin treatment (1 mM), see figure 3.11. From 1 mM to 5 mM treatment the viability decreases a lot in week 1, but from 5 mM to 10 mM the viability decreases less in this assay. The second assay (week 2) have a continuously linear decrease in cell viability from the control with MQ-water to the 5 mM metformin treatment, but also here the curve flattens out going from 5 mM to 10 mM, see figure 3.11. The standard deviations were relatively low in the week 1 assay, but in the week 2 assay there was a lot of variation between the three parallels. The 1 mM wells in week 1 had the highest standard deviation, see figure 3.11.

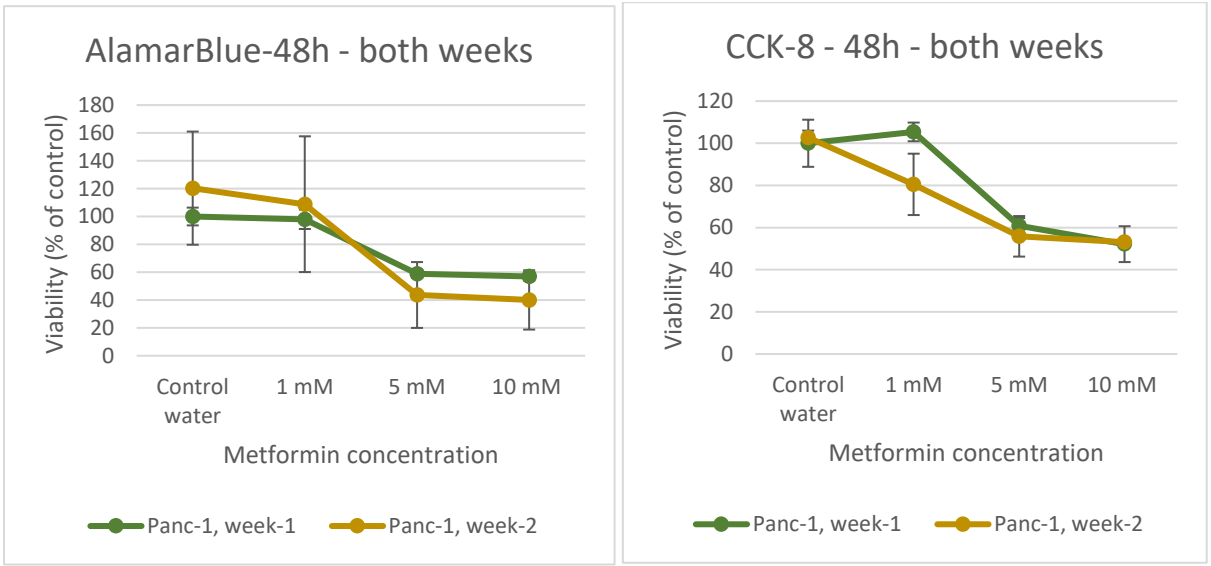

Figure 3.11: Results from cell viability assay of the Panc-1 cell line after 48 hours of metformin treatment

This figure shows two cell viability assays done on the Panc-1 cell line after treatment with 1 mM, 5 mM and 10 mM metformin for 48 hours normalized to control containing DMEM media only. The experiment was done twice, week 1 and week 2. For each week two 96-wells plates were prepared by seeding out 10 000 cell/ well of the Panc-1 cell line. There was prepared one control with DMEM media only (missing in week 1), and one with DMEM media and MQ-water. Positive control was added for the alamarBlue assay. Six parallels on each plate were treated with the different metformin concentration. Half of the parallels were treated with alamarBlue reagent, and the other three were treated with the CCK-8 cell viability reagent. The figure to the left shows the fluorescence measured at 540-590 nm after addition of alamarBlue reagent. The figure on the right shows the absorbance measured at 450 nm after addition of the CCK-8 reagent.

4. Disscussion

4.1 AlamarBlue cell viability assays

Week 1 assay MIA-Pa-Ca-2

This cell line had high concentration of cells, but some unexpected variation was observed, see figure 3.3. One should expect a rising cell viability from 10 000 to 30 000 cell/wells, but the results show a higher cell viability in the 10 00 cell/well than in the 15 000 cells/well. The cell viability also decreases continuously from the 20 000 cell/well to the 30 000 cell/well. This is most likely due to not mixing the cell suspension enough before seeding out on the plate. It can also be due to more proliferation in some wells than others. The standard deviations show some variations, but none of the parallels differed so much that they had to be removed.

Week 1 assay Panc-1

The results show that the Panc-1 assay from week 1 had very low cell density, see figure 3.3. This could be due to errors like seeding out less cells than 10 000 cell/well. There might have been done mistakes in calculations, probably in the first steps as there is a rising cell viability even if it has lower density than expected and compared to the MIA-Pa-Ca-2 cell line. Other errors can be that the cell suspension was not mixed properly so the cells sink to the bottom of the tube and hence is not transferred to the plate. The standard deviations show that there were relatively low variations in the parallels.

The Panc-1 was also lacking the two last columns on the plate (25 000 cell/well and 30 000 cells/well) as there was not enough cell suspension, see figure 3.3. When adjusting the concentration to 500 000 cell /ml after centrifugation, the volume of added medium was not enough to complete the plate due to low confluency in the flask when starting the experiment. The cells should not have been passaged at a low ratio the days before the experiment, but this was done.

Week 2 assay MIA-Pa-Ca-2

This assay went very well for the MIA-Pa-Ca-2 cell line and shows a continuously rising cell viability and have low standard deviations witch one exception in the 15 000 cell/well. Here there was some variation between the three parallels. These results show that the calculations and the techniques used when preparing the plate was done correct, see figure 3.4.

Week 2 assay Panc-1

In this assay the Panc-1 cell line had much higher density of cells compared to the first week. This implies that there was done mistakes in the first assay when seeding out the cells. This second assay had some unexpected values in the 10 000 cells well and the 30 000 cells well. This is most likely due to wrong techniques in pipetting and not being completely exact when making the dilutions. There is also a possibility that the cells have proliferated more in some wells than others, or proliferation have been inhibited by unknown contamination. From the wells with 15 000 cells to 25 00 cells there was a rising trend in cell viability, see figure 3.4.

Week 3 assay MIA-Pa-Ca-2

In this assay the MIA-Pa-Ca-2 cell line had a continuously rising cell viability. The largest standard deviation was seen in the three parallels containing 10 000 cells/well and 20 000 cells/well, see figure 3.5. This can be due to seeding out the suspension unevenly (not mixing enough) so that some of the wells contained less cells than others. It can also be contamination that prevents cell proliferation or not adding the same amount of the alamarBlue reagent.

Conclusion

The optimal seeding density was 10 000 cell/well for both cell lines and hence this concentration was used in the metformin experiment.

4.2 Metformin trial results

Both two cell lines MIA-Pa-Ca-2 and Panc-1 was affected by the metformin treatment as the cell viability decreased as the metformin treatment increased. The most effective treatment time was 48 hours. There were some deviations in the results, most likely due to errors done under preparation of the plates.

4.2.1 Mia-Pa-Ca-2

MIA-Pa-Ca-2 metformin trial discussion

With the result from these two weeks it looks like metformin have an impact on MIA-Pa-Ca-2 cells.

The 24-hour metformin treatment shows for both weeks, that there is little effect on viability, which could mean that the metformin has not started to affect the cells yet. It looks like the seeding out of the cells were even in each well. The differences from 1mM metformin to 5 mM metformin is not that big, but it is a small decrease. From 5 mM to 10 mM metformin it is a little bigger decrease but still not much. On the CCK-8 test it looks like the cells got more affects from the control with water than from 1 mM metformin, but de standard deviation is a little bigger from both weeks, especially week 2 and that can have affect on the result.

The 48-hour metformin treatment start the same and then it shows a deviation that increase in size until 5 mM and then decrease at 10 mM again. When the plate had incubated enough it was possible to see some deviation in the colors in the wells, and some closer look in the microscope shows as the picture says in the result that it was a bubble in the corner of one well and some strange growth on another well. It can indicate the bigger deviation in the result for the 10 mM wells because both deviations were therefrom.

From week 1 the standard deviation isn't visible in the graphs it's because they were so small. The standard deviation from week 2 are a little bit larger which can mean the either the cells weren't spread in the wells evenly or when alamarBlue/CCK-8 was added it wasn't mixed good enough so it wasn't equal spread in the wells. It is also hard to say if the cells were growing like that before the metformin was added or if it happened when metformin start to affect the cells, the wells were only checked after they had incubated.

In the CCK-8 assays there was bigger standard deviation than in the alamarBlue assays, this might be because CCK-8 is more sensitive than alamarBlue.

4.2.2 Panc-1

Panc-1 metformin trial discussion

Based on this experiment the Panc-1 cell line seems to be affected by metformin as the viability decreases when treated with metformin *in vitro*. The dose of metformin that decreased the cell viability the most was 10 mM. This seems to be a trend in most of the Panc-1 cell viability assays after addition of metformin. The most dramatic decrease in cell viability was shown going from 1 mM to 5 mM, but there was also some further decrease from 5 mM to 10 mM in most of the assays. Due to high variation and some errors done when preparing the plates, it will be hard to conclude this. More assays should be done before making a conclusion. From the results it shows that in the

alamarBlue assay week 2 and the CCK-8 assay week 1 the cell viability increases when treated with 1 mM metformin compared to the control. This does not seem logic as metformin is expected to decrease viability and does decrease viability in most of the results with 1 mM compared to control, hence this is most likely due to errors done when preparing the plate. There might have been seeded out more than 10 00 cell/well. When pipetting cell suspension into the wells the suspension should be mixed carefully with the pipette, so the cells does not sink to the bottom of the tube. This might cause this unexpected rise in cell viability as the control might have less cells then the wells treated with 1 mM metformin. Also, the cell proliferation might differ between the wells and cause variations. Other errors can be that the tube containing metformin mixed in medium was not mixed properly so the actual concentration of metformin was lower than 1 mM. The variation seen in the results, especially in the week 2 assays can also be caused by not mixing the metformin solution or the cell suspension enough.

All the week 1 assays lacked control with DMEM media only, but the week 2 assay showed that MQ-water had little effect on the cells, so this result was normalized to the MQ-water control. The plates that was treated for 48 hours had more decrease in viability than the ones treated for 24 hours, hence longer treatment time seems more effective. The week 1 alamarBlue assay had a relatively high increase in viability going from 5 mM to 10 mM, this can also be due to errors. In all the other assays the curve flattens out going from 5 mM to 10 mM metformin treatment. This induce that the most effective concentration of metformin is 5 mM for the Panc-1 cell line, based on these results. Other errors that might have affected the results is that there was not added enough reagent (alamarBlue/CCK-8). The reagent was mixed in DMEM media before it was added to the wells. If this solution was not properly mixed there can be variations in the concentration of added reagent which affect the results. When adding the CCK-8 reagent there was a small bubble in the week 1 48 hours plate. This can cause errors when measuring absorbance. There can also have been contaminations like small particles from clothes etc. that can have affected the behavior of the cells and hence the results.

MIA-Pa-Ca-2 and Pan-1 are affected by metformin treatment

Both cell lines were affected by the drug, but the MIA-Pa-Ca-2 cell line had the most decrease in viability when treated with metformin. The MIA-Pa-Ca-2 also had lower standard deviations compared to the Panc-1 and had a more accurate trend in the results. This was most likely due to more errors done when executing the experiments for the Panc-1 cell line.

This is a good indication that metformin can work as a cancer treatment but results like these alone are far from enough to conclude if it is worth using metformin on cancer patients. Cells kept in vitro in a controlled environment like the cell lines in this experiment may act very different then the same cell lines in vivo, in tumors. The human body are highly complex and cells in the body are a part of a signaling network that affect the cells, hence differently than cells kept in vitro. In vivo experiments are needed to find out if a drug can be used for certain purpose or not.

Metformin on the other hand is a drug that are already approved for medical use as it is widely used to treat type 2 diabetes. It is considered highly safe and with little side effects. This makes it easier to do human trials to see if the drug might have other beneficial effects than the already known effects. Metformin is widely studied and there are numerous of published scientific articles on its effects, many of these are studies on metformin's effect on cancer. In this project 66 different scientific articles on metformin's effect on various types of cell lines were included, and most of these articles focused in on cancer. Many of these articles concluded that metformin might have a beneficial effect on cancer cells.

4.3 Database creation and machine learning

Extracting information from previous experiments can be a good way to improve one's own research and can be a way to validate results as well as getting new knowledge on a subject. As done in this experiment, extracting what information we though would be important, and organizing it so it could be applied to a machine learning algorithm is a very effective way to store knowledge and also make predicting models based on the previous experiments done. As beginners in the machine learning and coding world the model made in this project did not give good predictions, but if correctly done, this way of doing research might be the future.

The knowledge is out there, finding good sources on metformin's effect on cancer cells was not difficult. What was challenging was extracting the information and get it ready for the machine learning part. Using machine learning and artificial intelligence to improve research seems to be the future as the technology improves rapidly. Maybe there should be a golden standard for how to design a publishment, so it is more appliable for machine learning algorithms? And making an online machine learning library of extracted information on different subjects could be very useful. Articles that are already published should also be in this library so there is lots of work needed to make this possible.

5. Conclusion and future perspectives

From this experiment alone the conclusion is that metformin does influence pancreatic cancer cell lines as it decreases their viability. Based on the results from this experiment the dosage that seemed to have the best effect on both cell lines was 10 mM metformin and the most effective treatment time for decreasing viability was 48 hours.

Experiments like the ones done in this project is a useful tool when testing drugs as there is no risk factor as in experiments done on animals or humans. To further test metformin effect in pancreatic cancer cell line the experiment should have been done several times, but there was not time for this in this project.

When it comes to metformin and its effect on cancer, one could use machine learning to predict how different cancer cells will be affected by the drug, in vitro and in vivo. To get the best predictions one should gather as many as possible of previous experiments and knowledge and have someone capable of creating a good machine learning model. The predictions of the model should also be verified upon results of traditional experiments, and should not be used to make decisions alone, but be a tool for improving decisions.

Also, it could be interesting to create a model that simulates the human body and tumors, this could be very helpful when testing new medicines and treatments. This might be very challenging because the human body is highly complex, and all its functions are not fully understood yet, but this kind of models could contribute to more effective and safe testing of new drugs. Computers are extremely effective and can run many tests simultaneously, including previously research. A problem with this kind of models is that researchers might discover new functions of the human body and then the model can be wrong, but if the model is used as a tool combined with standard research methods, these errors can be discovered. Humans can react different to treatments as well, so the model might not fit for everyone, but still would be a useful tool in general. Models could also be personalized to a specific disease and specific tumors. Machine learning seems to be more used in many different fields as well as in science and holds very interesting possibilities for the future.

6. Publication bibliography

ABP Biosciences (2021): Cell-Quant™ AlamarBlue Cell Viability Reagent | ABP Biosciences. Available online at https://www.abpbio.com/product/cell-quant-alamarblue-cell-viability-reagent/, updated on 5/10/2021, checked on 5/10/2021.

Agilent (2020): How Agilent Seahorse XF Analyzers Work | Agilent. Available online at https://www.agilent.com/en/products/cell-analysis/how-seahorse-xf-analyzers-work, updated on 3/19/2020, checked on 5/10/2021.

BMGLabtech.com (2021a): Absorbance, updated on 5/10/2021, checked on 5/10/2021.

BMGLabtech.com (2021b): Microplate Reader | Plate Reader - BMG LABTECH. Available online at https://www.bmglabtech.com/microplate-reader/, updated on 5/10/2021, checked on 5/10/2021.

Camacho, Diogo M.; Collins, Katherine M.; Powers, Rani K.; Costello, James C.; Collins, James J. (2018): Next-Generation Machine Learning for Biological Networks. In *Cell* 173 (7), pp. 1581–1592. DOI: 10.1016/j.cell.2018.05.015.

Chen, Kailin; Li, Yajun; Guo, Zhen; Zeng, Yong; Zhang, Wei; Wang, Hui (2020): Metformin: current clinical applications in nondiabetic patients with cancer. In *Aging* 12 (4), pp. 3993–4009. DOI: 10.18632/aging.102787.

Ecancer (2021): Innovative approaches for cancer treatment: current perspectives and new challenges - ecancer. Available online at https://ecancer.org/en/journal/article/961-innovative-approaches-for-cancer-treatment-current-perspectives-and-new-challenges, updated on 5/10/2021, checked on 5/10/2021.

Expert.ai (2020): What is Machine Learning? A definition. Available online at https://www.expert.ai/blog/machine-learning-definition/, updated on 5/3/2021, checked on 5/10/2021.

Handelman, G. S.; Kok, H. K.; Chandra, R. V.; Razavi, A. H.; Lee, M. J.; Asadi, H. (2018): eDoctor: machine learning and the future of medicine. In *Journal of Internal Medicine* 284 (6), pp. 603–619. DOI: 10.1111/joim.12822.

Heinz, Sabrina; Freyberger, Alexius; Lawrenz, Bettina; Schladt, Ludwig; Schmuck, Gabriele; Ellinger-Ziegelbauer, Heidrun (2017): Mechanistic Investigations of the Mitochondrial Complex I Inhibitor Rotenone in the Context of Pharmacological and Safety Evaluation. In *Sci Rep* 7 (1), p. 45465. DOI: 10.1038/srep45465.

Khan Academy (2021): Steps of cellular respiration | Biology (article) | Khan Academy. Available online at https://www.khanacademy.org/science/ap-biology/cellular-energetics/cellular-respiration-ap/a/steps-of-cellular-respiration, updated on 5/10/2021, checked on 5/10/2021.

Kroemer, Guido; Pouyssegur, Jacques (2008): Tumor cell metabolism: cancer's Achilles' heel. In *Cancer Cell* 13 (6), pp. 472–482. DOI: 10.1016/j.ccr.2008.05.005.

Liberti, Maria V.; Locasale, Jason W. (2016): The Warburg Effect: How Does it Benefit Cancer Cells? In *Trends in biochemical sciences* 41 (3), pp. 211–218. DOI: 10.1016/j.tibs.2015.12.001.

Lifeline Cell Tech Team (2020): Lifeline Cell Culture Media Produces Optimal Results. In *Lifeline Cell Technology*, 1/10/2020. Available online at https://www.lifelinecelltech.com/lifelines-cell-culture-media-produces-optimal-results/, checked on 5/12/2021.

Luminex Corporation (2020a): Muse® Count & Viability Kit 200X. Available online at https://www.luminexcorp.com/muse-count-viability-kit-200x/#overview, updated on 10/9/2020, checked on 5/10/2021.

Luminex Corporation (2020b): Muse® Count & Viability Kit 200X. Available online at https://www.luminexcorp.com/muse-count-viability-kit-200x/#documentation, updated on 10/9/2020, checked on 5/10/2021.

Luminex Corporation (2021): Guava Muse Cell Analyzer - Luminex Corporation Flow Cytometry. Available online at https://www.luminexcorp.com/muse-cell-analyzer/#overview, updated on 1/21/2021, checked on 5/10/2021.

Lv, Ziquan; Guo, Yajie (2020): Metformin and Its Benefits for Various Diseases. In *Frontiers in endocrinology* 11, p. 191. DOI: 10.3389/fendo.2020.00191.

Maria Ahmad; Adam Wolberg; Chadi I. Kahwaji (2020): Biochemistry, Electron Transport Chain. In Maria Ahmad, Adam Wolberg, Chadi I. Kahwaji (Eds.): StatPearls [Internet]: StatPearls Publishing. Available online at https://www.ncbi.nlm.nih.gov/books/NBK526105/.

Martin, N. C.; Pirie, A. A.; Ford, L. V.; Callaghan, C. L.; McTurk, K.; Lucy, D.; Scrimger, D. G. (2006): The use of phosphate buffered saline for the recovery of cells and spermatozoa from swabs. In *Science & Justice* 46 (3), pp. 179–184. DOI: 10.1016/S1355-0306(06)71591-X.

Medicalnewstoday (2020): pancreatic-cancer-affects-the-pancreas.jpg (1100×794), updated on 7/15/2020, checked on 5/10/2021.

MedlinePlus Medical Encyclopedia (2021): Cancer treatments: MedlinePlus Medical Encyclopedia. Available online at https://medlineplus.gov/ency/patientinstructions/000901.htm, updated on 5/5/2021, checked on 5/10/2021.

National Cancer Institute (2021a): Pancreatic Cancer Treatment (Adult) (PDQ®)–Patient Version. Available online at https://www.cancer.gov/types/pancreatic/patient/pancreatic-treatment-pdq, updated on 5/5/2021, checked on 5/10/2021.

National Cancer Institute (2021b): What Is Cancer? Available online at https://www.cancer.gov/about-cancer/understanding/what-is-cancer, updated on 5/7/2021, checked on 5/10/2021.

Nature (2021): Milestones in cancer. Available online at https://www.nature.com/immersive/d42859-020-00083-8/index.html?utm_source=facebook&utm_medium=social&utm_campaign=mile-cancer&utm_content=int&fbclid=IwAR2lPrGsLg8c5I5L5FQh8yiYSL8Oidh6sMRaAeY8laKN51T5DanW8X6NfZs%2Baem_AUl2o-pH6dmoHwKxOjxJ6b7OiGq2t9tODv2mHgUEoOaRQFqN7ixhLr5Q0NBlZBCdgTRuWIbfk_csoKwxCcAD9RIXVhiz61ql4lZHzBsDeqotaA, updated on 2/4/2021, checked on 5/10/2021.

Phd, Jean-françois Têtu (2016): Still using MTT or WST-1 for cell counting? In *tebu-bio*, 5/20/2016. Available online at https://www.tebu-bio.com/blog/2016/05/20/still-using-mtt-or-swt-1-for-cell-counting/, checked on 5/10/2021.

PubChem (2021): Metformin. Available online at https://pubchem.ncbi.nlm.nih.gov/compound/Metformin#section=2D-Structure, updated on 5/10/2021, checked on 5/10/2021.

Rampersad, Sephra N. (2012): Multiple applications of Alamar Blue as an indicator of metabolic function and cellular health in cell viability bioassays. In *Sensors (Basel, Switzerland)* 12 (9), pp. 12347–12360. DOI: 10.3390/s120912347.

Rawla, Prashanth; Sunkara, Tagore; Gaduputi, Vinaya (2019): Epidemiology of Pancreatic Cancer: Global Trends, Etiology and Risk Factors. In *World journal of oncology* 10 (1), pp. 10–27. DOI: 10.14740/wjon1166.

Rena, Graham; Hardie, D. Grahame; Pearson, Ewan R. (2017): The mechanisms of action of metformin. In *Diabetologia* 60 (9), pp. 1577–1585. DOI: 10.1007/s00125-017-4342-z.

Saraei, Pouya; Asadi, Ilia; Kakar, Muhammad Azam; Moradi-Kor, Nasroallah (2019): The beneficial effects of metformin on cancer prevention and therapy: a comprehensive review of recent advances. In *Cancer management and research* 11, pp. 3295–3313. DOI: 10.2147/CMAR.S200059.

Sarnecka, Agnieszka K.; Zagozda, Malgorzata; Durlik, Marek (2016): An Overview of Genetic Changes and Risk of Pancreatic Ductal Adenocarcinoma. In *Journal of Cancer* 7 (14), pp. 2045–2051. DOI: 10.7150/jca.15323.

Store medisinske leksikon (2021): trypsin – Store medisinske leksikon. Available online at https://sml.snl.no/trypsin, updated on 5/10/2021, checked on 5/10/2021.

Vial, Guillaume; Detaille, Dominique; Guigas, Bruno (2019): Role of Mitochondria in the Mechanism(s) of Action of Metformin. In *Frontiers in endocrinology* 10, p. 294. DOI: 10.3389/fendo.2019.00294.

Warburg, O.; Wind, F.; Negelein, E. (1927): THE METABOLISM OF TUMORS IN THE BODY. In *The Journal of general physiology* 8 (6), pp. 519–530. DOI: 10.1085/jgp.8.6.519.

Zhang, Wen; Zhang, Shao-Lin; Hu, Xiaohui; Tam, Kin Yip (2015): Targeting Tumor Metabolism for Cancer Treatment: Is Pyruvate Dehydrogenase Kinases (PDKs) a Viable Anticancer Target? In *International Journal of Biological Sciences* 11 (12), pp. 1390–1400. DOI: 10.7150/ijbs.13325.

Zhou, Qiao; Melton, Douglas A. (2018): Pancreas regeneration. In *Nature* 557 (7705), pp. 351–358. DOI: 10.1038/s41586-018-0088-0.